Published in IEEE Transaction on Electromagnetic Compatibility,
vol.56, no.4, pp.854,863, 2014,

HIRF Virtual Testing on the C-295 Aircraft: On the Application of a Pass/Fail Criterion and the FSV Method

Guadalupe G. Gutierrez, Jesus Alvarez, *Student Member, IEEE*, Enrique Pascual-Gil, *Member, IEEE*, Mauro Bandinelli, Rodolfo Guidi, Valerio Martorelli, Mario Fernandez Pantoja, *Senior Member, IEEE*, Miguel Ruiz Cabello, and Salvador G. Garcia, *Member, IEEE*

***Abstract*—In this paper, we show the application of numerical simulation for the virtual testing of a very complex system under high-intensity radiated fields (HIRF) conditions. Numerical results have been compared to measurements performed on a C-295 aircraft. The approach is based on the use of multiple tools for the preprocessing, computation, and postprocessing, all of them integrated under the same framework. This study is a part of the HIRF SE project, and the final step for the validation of the tools involved there, to introduce the use of simulation in the whole aircraft certification process in an HIRF environment. The main goal of the project is to provide the aeronautic industry with a numerical modeling computing framework, which could be used to predict the electromagnetic performance, and to carry out parametrical studies during the design phase, when changes are simpler and less costly. It could also lead in the future to a considerable reduction on the certification/qualification testing phase on air vehicles, to cross validate the results obtained from measurement and simulation providing best confidence in them, and to attain a more exhaustive analysis to achieve a higher level in the air vehicle safety.**

***Index Terms*—Electromagnetic (EM), electromagnetic compatibility (EMC), feature selective validation (FSV), finite difference time domain (FDTD), high-intensity radiated fields (HIRF), low-level swept fields (LLSF), oversized cavity theory (OCT), perfect electric conductor (PEC), radio frequency (RF), time domain analysis.**

I. Introduction

THE increment in the use of electronics and complexity in modern aircrafts, and the expanded use of the spectrum worldwide, makes the topic of susceptibility under high-intensity radiated fields (HIRF) conditions a key issue for the certification of any air vehicle. The traditional approach to tackle this electromagnetic compatibility (EMC) problem is based mainly on testing. This approach presents some limitations due to the complexity of the systems, sizes, and strong requirements, defined in terms of frequency bands and electrical field levels [1]. The development of efficient algorithms and methods able to deal with electrically large structures, and the exponential growth of computational capabilities, make it possible to estimate transfer functions between incident electromagnetic (EM) fields and internal fields, or induced currents on bundles. This technology, not only can save a lot of time and cost in the certification process of an aircraft, but it can also be very useful during the whole life of a system; design, development, certification, upgrading or maintenance phases, increasing the safety of the current approach.

In this context, the European FP7 HIRF-SE project [2] is intended to provide the aeronautics industry with a synthetic environment integrated by a numerical simulation tool set (finite difference time domain (FDTD), method of moments (MoM), multitransmission line network (MTLN), material modeling tool (MMT), etc.), preprocessing tools, such as meshers, and postprocessing tools (FFT, filters, feature selective validation (FSV) tool, etc.). This project agglutinates 44 partners, including airframers, national certification agencies, test-houses, commercial and university software houses, etc. One output of the project is a group of tools that work inside the same framework providing two key capabilities. On one hand, the tools can exchange data to perform the different phases of a specific simulation. On the other hand, the results from each particular tool can be used as inputs for other solvers in order to perform a better suited simulation to take into account the complexity of a real scenario.

The frequency spectrum of HIRF threats ranges from 10 kHz–40 GHz. Below 400 MHz, the dominant effect comes from the excitation of airframe resonances, inducing currents on the cable bundles of the aircraft. The penetration of the electric field into the equipment bays via gaps, seams, RF transparent materials. and apertures in the airframe structure and equipment enclosures, begins to increase its influence above 100 MHz. This energy, coming from the bundles into the equipments in the first case, or EM fields at wavelengths comparable to the equipment sizes in the second one, interacts directly with the avionics, being a source of malfunctions.

Manuscript received July 25, 2013; revised September 30, 2013; accepted October 29, 2013. This work was supported by the funding from the European Community Seventh Framework Programme FP7/2007-2013, under Grant 205294 (HIRF SE project), from the Spanish National Projects TEC2010-20841-C04-04, CSD2008-00068, from the Junta de Andalucia Project P09-TIC-5327, and from the Granada Excellence Network of Innovation Laboratories (GENIL) project.

G. G. Gutiérrez and E. Pascual-Gil are with Airbus Military, EADS Construcciones Aeronáuticas S.A., 28906 Getafe, Spain (e-mail: Guadalupe.Gutierrez@military.airbus.com; Enrique.Pascual@military.airbus.com).

J. Alvarez is with the Cassidian, EADS Construcciones Aeronáuticas S.A., 28906 Madrid, Spain (e-mail: jesus@ieee.org).

M. Bandinelli, R. Guidi, and V. Martorelli are with the IDS, Ingegneria dei Sistemi, 56121 Pisa, Italy (e-mail: m.bandinelli@idscorporation.com; r.guidi@idscorporation.com; v.martorelli@idscorporation.com).

M. F. Pantoja, M. R. Cabello, and S. G. Garcia are with the Department of Electromagnetism, University of Granada, 18071 Granada, Spain (e-mail: mario@ugr.es; mcabello@ugr.es; salva@ugr.es).

Color versions of one or more of the figures in this paper are available online at http://ieeexplore.ieee.org.

Digital Object Identifier 10.1109/TEMC.2013.2291680

A validation road map has been defined inside the HIRF-SE project, to assess the capabilities of the different tools and methods, and to ensure their correct application. This road map is based on three levels. In the first level, numerical test cases have been defined and solved with different methods and tools, finding basically code-to-code cross comparison and validation [3]–[6]. The second step is based on checking the validity of the codes to simulate more complex test cases, some of them representing real configurations, such as aeronautic structures, materials and bundles, by comparing experimental data with numerical results [7]–[9]. And finally, the third level performs a final validation by comparisons of results on real air vehicle test cases, and also addresses the application of the HIRF-SE framework in a certification process.

In this study, we present the final step where some of the methods and tools, already validated at first and second levels under HIRF-SE, are applied on a real aircraft. For that purpose, we use the Airbus Military C-295, for which low-level swept fields (LLSF) measurements exist.[1] We compare with simulation results found with two numerical methods to address the full frequency band: the FDTD tool by the UGR (UGRFDTD) [11] for low and intermediate frequencies, and a power balance [12], [13] technique by IDS (IDSOCT) for high frequency. Results serve to validate the road map defined under the HIRF-SE project for HIRF assessment by numerical techniques. Whenever the simulation results are good or conservative, they could be used for reducing the amount of tests during a certification process.

The rest of the paper is organized as follows. First, a description of the C-295 aircraft and details about the starting point and available information is presented, regarding measurements and CAD information. Second, details about the EM numerical modeling of the problem are provided. Finally, we show a comparison of measurements and simulations, applying both HIRF-SE pass/fail criterion and the IEEE standard FSV method [14].

II. Description of the Problem

The C-295 aircraft is a medium-weight transport aircraft, certified FAR-25 by FAA, the DGAC and the INTA airworthiness authorities. The airframe structure is mainly metallic, providing the first layer of protection from external EM sources. Each individual conductive structure component is required to have a low-impedance electrical bond in order to maintain an electrically homogeneous structure. Leakage of EM fields and currents may still occur due to apertures around hatches, joints, hinges and use of nonconductive materials in components such as windows, radomes, and fairings.

[1]LLSF procedure is used to measure the transfer function relating external RF fields to the internal RF fields. The test is conducted for several aircraft orientations and field polarizations to produce the worst case of the transfer functions for the bay being illuminated. These transfer functions can then be scaled to predict the field environment when the aircraft is exposed to the appropriate external HIRF environment to assess whether the internal HIRF electric fields comply with the specifications for maximum levels of the integrated systems [1], [10].

Fig. 1. LLSF tests at airbus military open-area test-site facility.

Airbus Military

Fig. 2. Electric field measurements during LLSF tests.

Q1

The materials in use in the C-295 aircraft are standard aeronautic materials. The main conductive materials used (compliant with [15]) are as follows:

1) aluminum alloys: 2024, 6061, 7075, 7050;
2) ferrous alloys: DAISI 4340, AISI 321, PH 13-8Mo;
3) titanium alloys: Ti6Al4V.

Additionally, composite materials are also used in the aircraft manufacturing such as carbon fiber and fiberglass (e.g., the radome is a *sandwich*-type structure with outer fiberglass laminates).

The LLSF test was performed in an open-area test-site (OATS) facility, by illuminating the aircraft with antennas for the frequency band between 100 MHz and 18 GHz. The aircraft is positioned in a location at least as far as 50 m from any source of electrical or electromechanical noise, and far away from any obstacle that can produce any undesired reflection (see Fig. 1).

(see Figs. 1 and 2).

A. Measurements

Measurements of LLSF according to EUROCAE ED-107 [1], [10] have been performed by Airbus Military personnel in their

OATS facility located in Getafe (Spain). It is a circular platform 90 m in diameter made of concrete with an embedded metallic ground plane.

Before the test, the electric field level has been measured at the observation points but without the aircraft, obtaining the calibration field level. Then, the aircraft has been placed at the OATS and the electric field level at six test points have been measured and normalized to the calibration field. Two test points are located in the cockpit, three in the cargo bay and one in the engine. Each zone has been illuminated from several angles and two polarizations so as to find the worst possible scenario, with regard to the energy coupling through apertures or slots. The worst case results from all illumination angles, both polarizations, and the points located at the same zone, have been calculated.[2] The attenuation transfer functions for each zone have been used to be compared with the simulation results.

B. CAD Data and Defeaturing

The model is obtained from the aircraft digital mock up. An image of the C-295 digital mock-up can be seen in Fig. 3(a). However, the complexity of the full CATIA (computer-aided three-dimensional interactive application, property of Dassault Systèmes) model is unaffordable and unnecessary for EM simulation purposes. Therefore, a simplification is needed to get a model simple enough to be meshed and computed, retaining all the internal/external details to be representative from the EM point of view. Taking that into account, the simplification is a crucial task consisting in the elimination of very small parts and details like holes, bolts, or nuts, or the redefinition of complex surfaces, for which the engineer experience plays a fundamental role [16]. Fig. 3(b) illustrates the result of the simplification process in the C-295 aircraft. Whereas the original model size is around 14 GB (unmanageable for an average PC), the simplified model is around 30 MB, small enough to be manipulated in a PC, and, at the same time, containing all the relevant details so as to be electromagnetically representative.

Since the C-295 aircraft is mainly made of metallic materials, it can be considered for EM simulations as perfect electric conductor (PEC) surfaces. Engine nacelles are made of a multilayered carbon fiber with aluminum foil which has been modeled as PEC with perfect continuity between panels, since it has a high shielding effectiveness, and the main entry points of these cavities are other than the connections between different pieces. The same approach has been considered for other parts made of carbon fiber or fiber glass with aluminum foil located in the center wing, the landing gear sponsons or small pieces in the stabilizers or wings. The total amount of composite materials composing the C-295 aircraft is no more than 20%. Dielectrics with no losses, such as fiberglass parts, have been eliminated from the EM model. For high-frequency simulations performed with OCT, some absorbing volumes have been introduced as a model for the seats in the cockpit, and for the nonmetallic pipes in the engine.

[2]This is the maximum value frequency-by-frequency of all the curves under consideration, resulting the envelope of all of them.

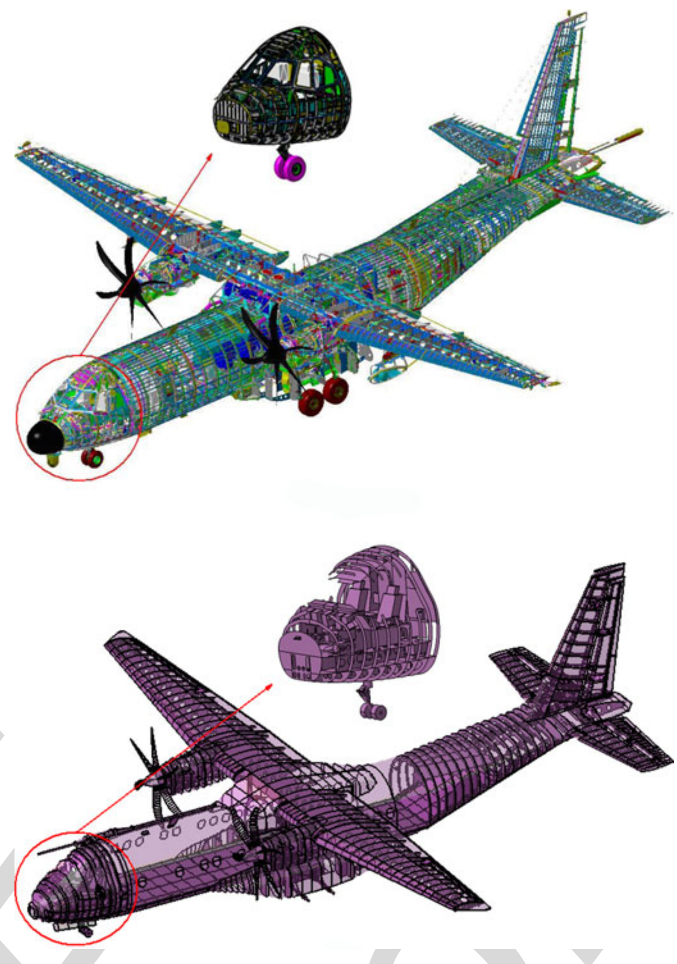

Fig. 3. (a) Isometric view of the C-295 digital mock-up with a detailed view of the cockpit. (b) C-295 simplified geometry with a detailed view of the cockpit (aerodynamic surfaces are depicted with a degree of transparency to allow the observation of the internal surfaces).

This simplified model made of metallic surfaces has been used for low-medium frequency simulations carried out with FDTD method between 100 MHz and 1 GHz. It has also been used in order to easily extract the volumes and surfaces required by power balance technique to perform high-frequency simulations between 1 and 18 GHz.

III. EM Modeling

Following the road-map defined inside the HIRF-SE project, numerical models of the C-295 aircraft have been prepared to work with the UGRFDTD code for low and medium frequencies and the IDSOCT code for high frequencies. A validation of the obtained results has been performed with respect to experimental data.

A. Low-Medium Frequency Model

The UGRFDTD [11] code has been used for simulating the frequency range between 100 MHz and 1 GHz. It is a time-domain 3-D full-wave method based in Yee classical FDTD method [17] with MTLN extensions for cable bundle treatment

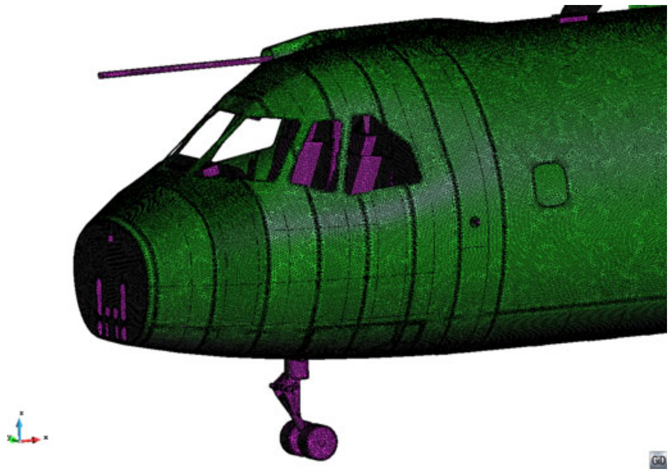

Fig. 4. C-295 cockpit unstructured mesh.

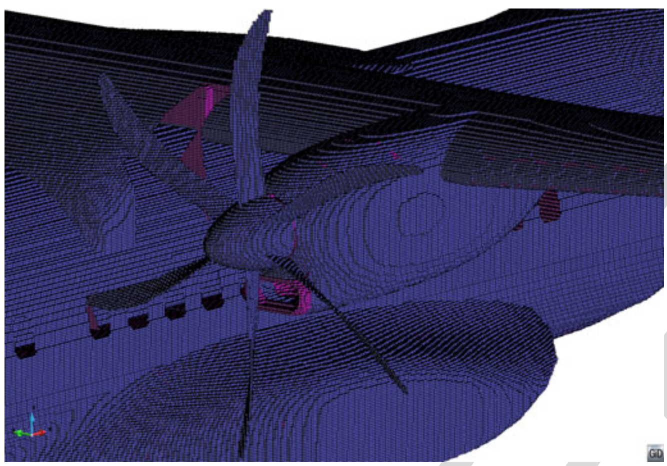

Fig. 5. Cartesian mesh of the engine and central fuselage external geometry.

[18]. The model has been built using GiD [19] and NASH [20] utilities. Further details of these (and other) tools used for the simulations are beyond the scope of this paper and provided in the references.

The first step consists on generating IGES files from the simplified CAD models, which are imported into GiD to obtain an unstructured mesh. In this case, a size of 20 mm has been used for the unstructured mesh.[3] A detailed view of the C-295 cockpit unstructured mesh appears in Fig. 4.

Second, from the unstructured mesh, a Cartesian mesh with uniform space steps in the three directions is created by using the NASH FDTD mesher. Reaching a compromise is necessary to select the cell size since it should be small enough to represent properly the relevant details of the structure and to solve the highest frequency of interest, and big enough to have a computationally affordable number of cells. In this case, a cell size of 20 mm has been selected, which has led to a total size of the grid of 734 Mcells ($1228 \times 1307 \times 459$). The quality of the Cartesian mesh can be seen in Fig. 5.

[3]Triangular elements are required (2087909 triangles in total) for PEC surfaces.

Finally, a simulation for each configuration is performed using the UGRFDTD code [11]. The time step has been selected at 80% of the Courant–Friedrichs–Lewy stability condition (30 ps) [21]. The space and time steps properly sample wavelengths and frequencies up to 1 GHz. The observables have been recorded for each time step. The boundary conditions have been set to perfect matching layer (PML) with eight cells, except for the lower Z-plane, where a PEC condition has been used to model the metallic ground plane of the OATS facility. The waveform of the plane wave illuminating the aircraft has been a modulated Gaussian pulse.

Taking into account the relationship between the distance from the illuminating antennas to the aircraft (10 m), and the size of the aircraft area being illuminated, the incident field can be considered to be in the far field for the measured frequency band (100 MHz to 18 GHz). Therefore a plane-wave illumination can be used instead of the actual test setup, with the subsequent computational resources savings (a deeper discussion on this is found in [7]).

B. High-Frequency Model

The IDSOCT code has been used for simulating the frequency range between 1 and 18 GHz. This method is based on oversized cavity theory (OCT) which belongs to the power balance approaches applicable to high-frequency modeling of quasi-cavity enclosures [12], [13].

Provided that some conditions about frequency, volumes, and Q factor of the enclosure are satisfied, it is demonstrated that the internal EM field distribution is statistically homogeneous, and follows some known statistical distributions (depending on the observable).

IDSOCT verifies the existence of such conditions in all different regions of the model, and calculates the parameters of the statistical distributions at them. From these, it is possible to extract the data of interest for the EMC problem. IDSOCT defines the characteristics of all the cavities in the aircraft including their volume, surface of the walls, surface of apertures, external sources, lossy objects, etc. In general, the cavities correspond to the different compartments of the aircraft. The panels represent the walls of those compartments. The apertures are the different holes, gaps, slots, etc., on the walls connecting a compartment to other ones, or to the exterior. And, the lossy objects replace the lossy materials existing within each compartment.

For the C-295 aircraft, all the geometrical parameters have been obtained from the simplified model using the measurement tools provided by CATIA V5. The resulting model comprises 17 cavities, 89 panels, 175 apertures, and 23 lossy objects. An external source corresponding to an impinging plane-wave of 1 V/m has been applied to each exterior aperture being illuminated from each illumination angle and field orientation, with respect to the apertures. The compartments where the field has been measured are the cockpit, the cargo bay, and the engine (the rest of the cavities have also been included, to take into account the connections between those ones, and/or to the exterior).

IV. Pass/Fail Criterion

A pass/fail criterion (PFC) has been defined within the project consortium, taking into account the expertise of certification authorities, airframers, test-houses, and simulation experts [1], [10], and [2]. The application of this criterion can be summarized as follows.

1) A set of seven observation points occupying the volume of the receiving antenna is used to probe the EM field through an average operation. This process obtains a better representation of the receiving antenna used during the tests.
2) A minimum of 100 frequencies per decade above 100 kHz equally spaced on a log scale is measured.
3) The raw data is filtered by using an averaging bandwidth of 5% of the frequency of interest.
4) The maximum value frequency-by-frequency considering all illumination angles and both polarizations, for each point, is calculated, and taken as the worst case (WC) results.
5) The maximum values of the WC, within a sliding frequency window of 10% of the central frequency, are used to find the data envelopes. This permits to account for any shift in resonances between the aircraft installation and the modeled test setup.
6) Finally, the value of the difference between simulation and measurement in dB is calculated.
7) The data are assumed to pass the criterion if this difference falls below 6 dB.

This PFC has been applied to the solvers developed under the HIRF-SE project in last validation phase, together with the FSV method (later presented), in order to perform cross comparisons and draw conclusions on their validity and range of application.

A. PFC for Low-Medium Frequency[4]

The numerical results for the E-fields at each test point have been normalized by the incident field of the plane-wave so as to obtain the attenuation transfer functions. Those results have been extrapolated to 1 V/m since the observables are the electric field normalized to an incident field of 1 V/m at each test point.

Figs. 6–8 show some comparisons between the WC results of the measured data and the ones of the numerical results using the UGRFDTD code, and also the comparison between the envelopes resulting from the application of the sliding frequency window. It can be seen that measurement and computation envelopes are less than 6 dB apart for most of the frequencies.

Table I summarizes the results for all the six points analyzed according to the PFC. The quality of the simulations can be considered good since the mean difference is close to 0 dB and the main deviations are located in narrow frequency bands [see Figs. 6 and 7(b)].

[4]For all the graphs shown in this section, the vertical scale has been removed due to nondisclosure and intellectual property rights (the missing *y*-axis are always linear with ticks spaced by 0.1 V/m).

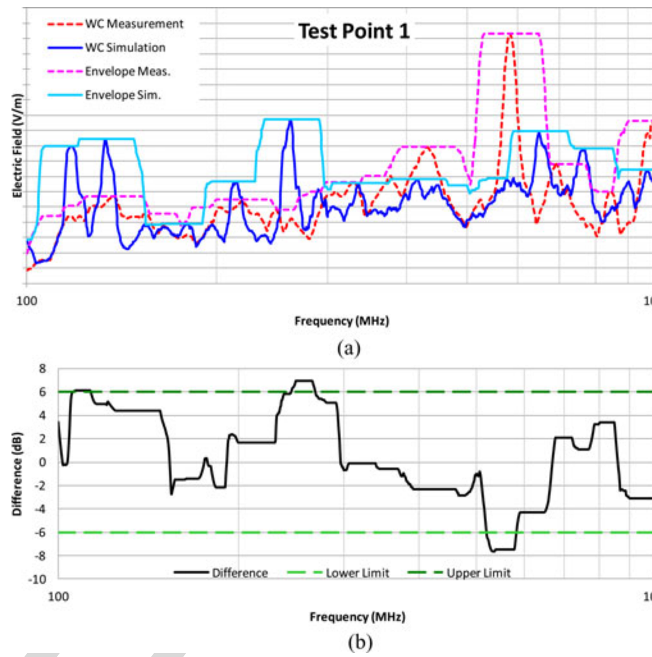

Fig. 6. (a) Comparison between measurements and simulations for the test point 1 located in the cockpit. (b) Difference between simulation and measurement and 6 dB limit.

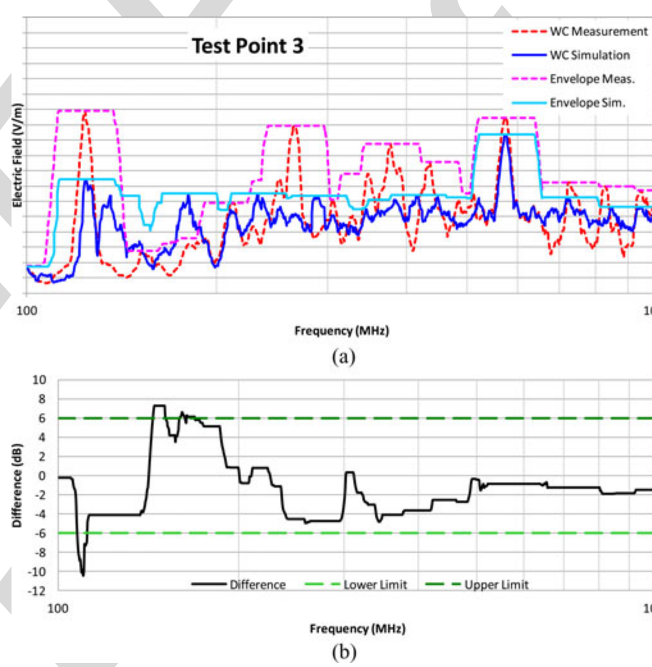

Fig. 7. (a) Comparison between measurements and simulations for the test point 3 located in the cargo bay. (b) Difference between simulation and measurement and 6 dB limit.

B. PFC for High-Frequency Results

For the high-frequency range, the shielding effectiveness at several points inside each cavity (for instance, the cockpit or the cargo bay) has been measured. Then, the mean values from all illumination angles, both polarizations and the points located at the same zone have been calculated and these transfer functions have been converted to E-field considering an illumination field

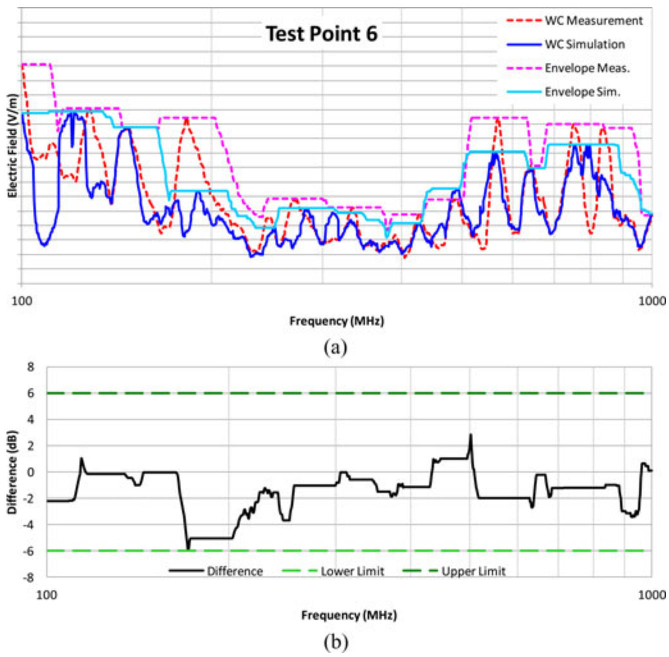

Fig. 8. (a) Comparison between measurements and simulations for the test point 6 located in the engine. (b) Difference between simulation and measurement and 6 dB limit.

TABLE I
PFC Results for the UGRFDTD Code

Pass/Fail Criterion	*Points Inside Limit*	*Greatest Difference*	*Mean Difference*
Test Point 1	88 %	-7.65	0.51
Test Point 2	89 %	16.29	1.03
Test Point 3	94 %	-10.44	-1.34
Test Point 4	81 %	-14.41	-2.52
Test Point 5	76 %	-12.20	-1.55
Test Point 6	100 %	-5.95	-1.41

Percentage of points inside the limit, greatest difference between envelopes and mean difference between envelopes.

TABLE II
PFC Results for the IDSOCT Code

Pass/Fail Criterion	*Points Inside Limit*	*Greatest Difference*	*Mean Difference*
Cockpit	96 %	-6.98	-1.99
Cargo Bay	94 %	-8.33	-1.72
Engine	100 %	-5.48	-2.38

Percentage of points inside the limit, greatest difference between envelopes and mean difference between envelopes.

of 1 V/m. For the simulations, the mean E-fields at each cavity for an incident field of 1 V/m have been found using IDSOCT. The mean values from all illumination angles and polarizations have been computed.

Figs. 9–11 show the comparison between the mean and envelope measured values (with the procedure described for the PFC to find the envelopes) and the numerical results using the IDSOCT code.

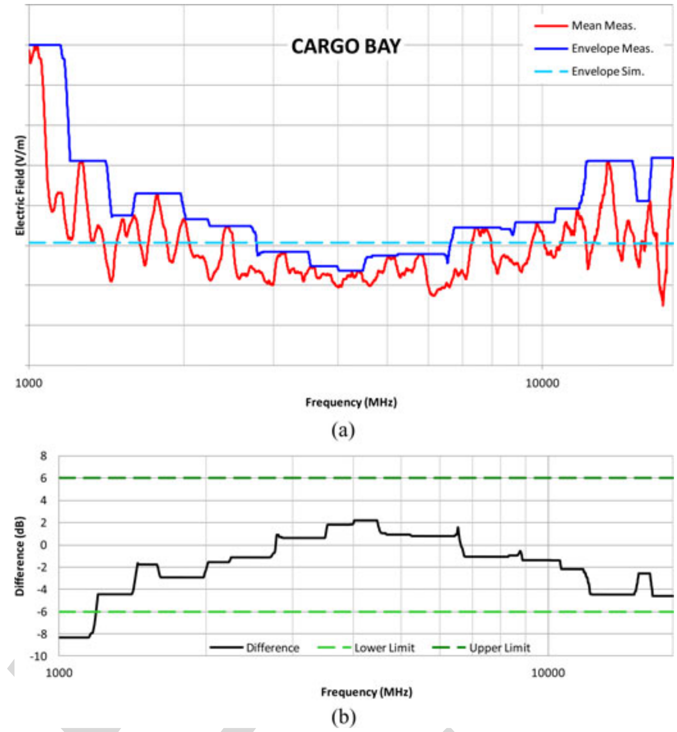

Fig. 9. (a) Comparison between measurements and simulations for the Cockpit. (b) Difference between simulation and measurement and 6 dB limit.

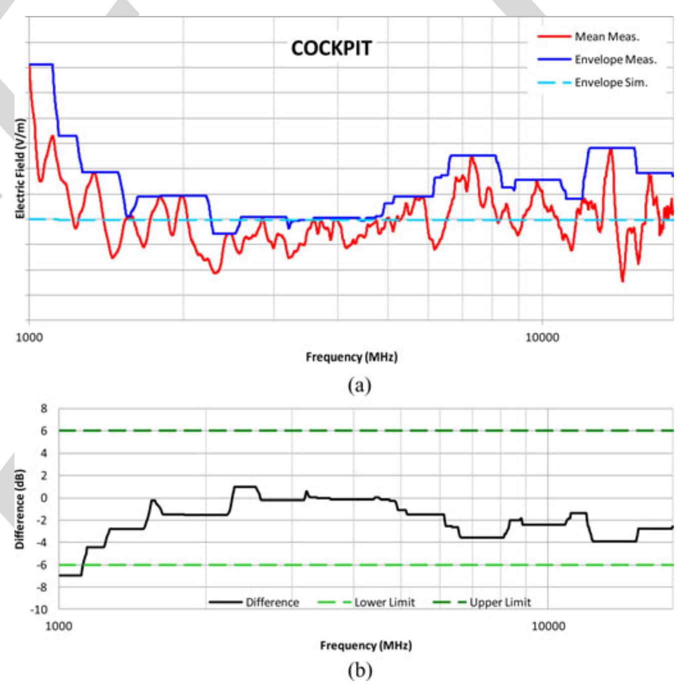

Fig. 10. (a) Comparison between measurements and simulations for the Cargo Bay. (b) Difference between simulation and measurement and 6 dB limit.

Table II summarizes the results for the three zones under study. Similar conclusions that for the low-medium frequency case are found.

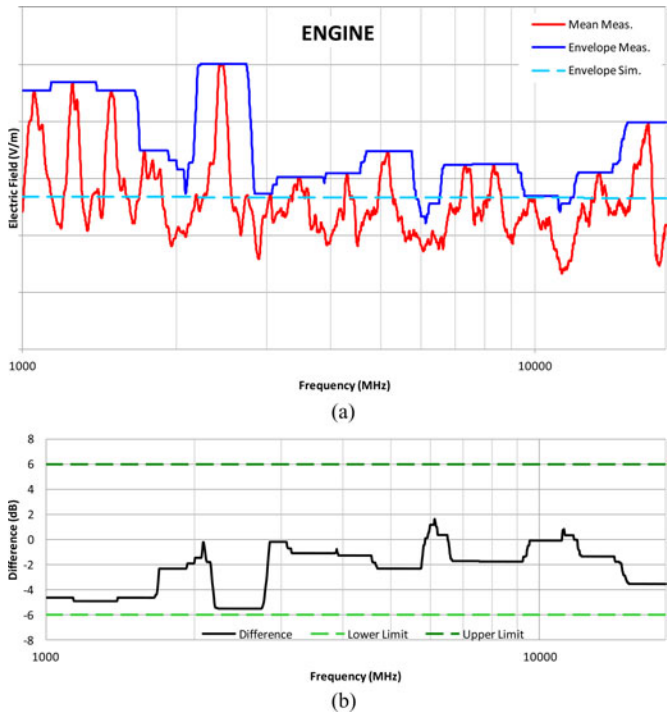

Fig. 11. (a) Comparison between measurements and simulations for the Engine. (b) Difference between simulation and measurement and 6 dB limit.

TABLE III
FSV Results for the UGRFDTD Code

FSV	GDM	ADM	FDM	Grade (G/A/F DM)	Spread (G/A/F DM)
Test Point 1	0.9936	0.6123	0.6880	5/5/5	3/4/5
Test Point 2	0.7764	0.4588	0.5796	5/4/5	4/4/5
Test Point 3	0.7689	0.4640	0.5572	5/5/5	4/4/5
Test Point 4	0.7943	0.5702	0.5042	5/5/5	3/4/5
Test Point 5	0.8357	0.4876	0.5682	5/5/5	4/5/5
Test Point 6	0.6295	0.3418	0.4934	5/4/5	4/4/5

V. Feature Selective Validation

One of the most widely used validation methods in EMC is the feature selective validation method (FSV) [22]–[25]. It was developed to take into account the expertise of engineers when assessing comparison of numerical/experimental data. It has been adopted by the IEEE standard 1597.1 [14]. In this paper, the FSV routine from the EMC Laboratory of the University of L'Aquila [26] has been used for this purpose.

The low-medium frequency simulation and measurement results have been analyzed with FSV. Fair agreements are obtained, in general, as seen in Table III. The actual WC curves have been employed now, instead of the envelopes used for the PFC, since they fit better to FSV methodology.

In order to provide a tentative correlation of the FSV and PFC ratings, let us use both methods to compare two sets of measurements, from two different test campaigns, performed with different C-295 aircrafts, and using different antennas and equipments. This comparison is helpful to find reference deviations in the comparison of two results. Fig. 12(a) depicts the result of the same data processing applied to two different attenuation measurements performed on a point in the cockpit.[5] Applying the PFC, the results shown in Fig. 12(b) and Table IV have been obtained, finding similar differences in both measurement/measurement and simulation/measurement comparisons in relation to the 6 dB limit.

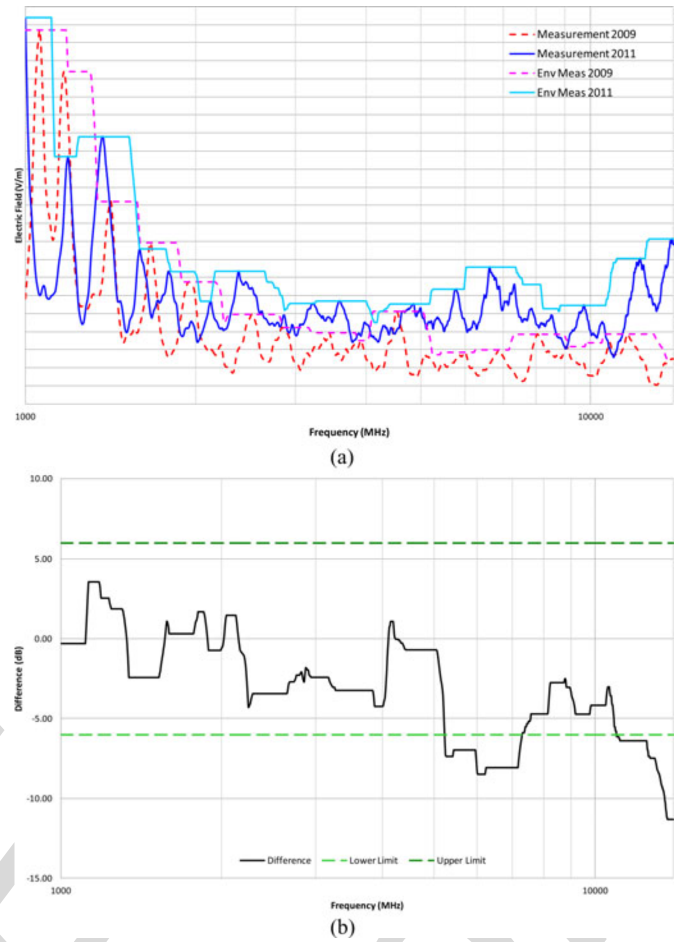

Fig. 12. (a) Comparison between two measurements on a point in the C-295 cockpit from different test campaigns. (b) Difference between the two measurements and 6 dB limit.

TABLE IV
PFC Results for Two Measurements From Different Test Campaigns

Pass/Fail Criterion	Points Inside Limit	Greatest Difference	Mean Difference
Point on cockpit	78 %	-11.33	-3.03

TABLE V
FSV Results for Two Measurements From Different Test Campaigns

FSV	GDM	ADM	FDM	Grade (G/A/F DM)	Spread (G/A/F DM)
Point on Cockpit	1.0232	0.8305	0.5663	5/5/5	3/3/5

The FSV rates for the measurement/measurement comparison are analyzed in Table V, revealing fair or even poor

[5]Only results for a single point in the cockpit were available to make this comparison (from 1000 to 14000 MHz).

agreement and high spread factors, as in the case of simulation/measurement comparison.

We can now extrapolate these PFC and FSV conclusions to the comparison of simulation with measurement data. For this case, like in the measurement/measurement one, fair or even poor agreement is found, while PFC finds matches within the 6 dB limit for most of the frequencies. It is inevitable to conclude that fair agreement for FSV could also be fully acceptable in both cases, since the uncertainty budget of simulations and measurements are in the same order of magnitude.

We must also note that the FSV results reveal a high spread factor for both comparisons. High values of spread factor are inherent in this kind of EMC comparisons for complex electrically large structures, with wide-frequency bands spanning over several decades. Wide typical deviations are due to the test procedure and the determination of the WC in shielding measurements. For this reason, we find points with excellent agreement, other ones with only good agreement and even points with poor agreement. A slight filtering is accepted by the standards, but the aim of the analysis is, generally, to capture the WC and not to average the results. Then, the comparisons must be made between curves with the aforementioned drawbacks.

VI. Conclusion

This paper shows a validation of a tool set that could help the aeronautical industry to predict the shielding effectiveness of aircrafts under HIRF conditions. Their application during the design, qualification, or certification phases, would lead to a significant reduction in both time and cost of the aircraft development, and to an improvement on the air vehicle safety.

Two numerical simulation tools (UGRFDTD and IDSOCT) have been validated using LLSF measurements for a complex aircraft (C-295). This test case is part of the final validation step of the HIRF-SE project, where most outstanding European airframers and EMC researchers participate. Both, the FSV method, and a novel PFC of ± 6 dB, for postprocessed raw data, to compare in terms of envelopes, have been employed and cross compared.

The hybrid approach presented in this paper, which is based on the combined use of an FDTD method for low-medium frequencies and a power balance technique for high frequencies, enables us to cover the whole frequency range required by HIRF certification authorities for LLSF test (from 100 MHz to 18 GHz). The use of the FDTD method can be extended up to higher frequencies depending on the available computational resources, hopefully up to frequencies for which the number of modes inside the geometry cavities is high enough to use the power balance technique with high accuracy. Then, the overlap of both methods permits us to predict the EM performance over the complete LLSF frequency band.

Simulation results show good agreement with measurements for those test points which are inside cavities with big apertures, where the main entry points are well defined, and the lossy objects are also well known. Differences found between 100 and 200 MHz are apparently due to the use of plane-wave illumination for this frequency range, where the far-field criterion is in its limit. In the high-frequency range, the deviations are located between 1 and 1.2 GHz because the number of modes inside the cavities at these frequencies is not high enough.

Regarding the PFC, we can state that, in general, the results differ less than 6 dB for most of the frequency range, as for the two measurements from different test campaigns. It means that 6 dB of difference is a tight requirement and the simulation results obtained in this study present good quality, and PFC is useful for validating the tools that have been used on a real and complex geometry.

As far as FSV method is concerned, both the quality and the reliability of the comparisons have been evaluated as low (since grade and spread factors are high) and the figures of merit show, in general, only fair agreement. Taking into account that it is also the case when comparing two measurements from different test campaigns, we can conclude that this kind of FSV results are inherent in that kind of EMC comparisons between wide frequency band signals, and therefore they can be very good results for that application.

The case analyzed in this paper has illustrated a correlation between the FSV method and the PFC, that may eventually help to revise the FSV standard, to provide rates closer to the experts evaluation for wide-frequency band EMC problems. Fair results with high spread factor have been proved to be acceptable in those applications. FSV would better mirror the PFC results by, for instance, giving less weight to the FDM value, even though ADM have high spread, and by giving more level of importance to the maximums when calculating the ADM.

The exercise shown in this paper is part of the demonstration of the utility and limits of numerical tools in HIRF assessment. It has provided a road map to create EM numerical models of test setups, suitable to replace some experimental testings by costless numerical simulations. The results of these validations are among to those currently being proposed to international aviation agencies to be accepted in certification air vehicles under HIRF conditions.

Acknowledgment

The authors would like to thank the whole HIRF-SE consortium, and especially those partners directly involved in the development of the PFC, used in this paper for the C-295 aircraft.

References

[1] *"Guide to Certification of Aircraft in a High Intensity Radiated Field (HIRF) Environment,"* EUROCAE ED-107, Mar. 2001.

[2] (2008). HIRF SE project. [Online]. Available: http://www.hirf-se.eu

[3] J. Alvarez, L. Angulo, M. Bandinelli, H. Bruns, M. Francavilla, S. Garcia, R. Guidi, G. Gutierrez, C. Jones, M. Kunze, J. Martinaud, I. Munteanu, M. Panitz, J. Parmantier, P. Pirinoli, Z. Reznicek, G. Salin, A. Schroder, P. Tobola, and F. Vipiana, "EV55: A numerical workbench to test TD/FD codes in HIRF EMC assessment," presented at the EUROEM Eur. Electromagn., Toulouse, France, 2012.

[4] J. Alvarez, L. Angulo, M. Bandinelli, H. Bruns, M. Francavilla, S. Garcia, R. Guidi, G. Gutierrez, C. Jones, M. Kunze, J. Martinaud, I. Munteanu, M. Panitz, J. Parmantier, P. Pirinoli, Z. Reznicek, G. Salin, A. Schroder, P. Tobola, and F Vipiana, "HIRF interaction with metallic aircrafts. A comparison between TD and FD methods," in *Proc. Int. Symp. Electromagn. Compat. EMC Eur.*, 2012.

[5] (2013). CEMEMC workshop. [Online]. Available: http://www.cememc.org
[6] J. Alvarez, L. D. Angulo, A. R. Bretones, and S. G. Garcia, "A leap-frog discontinuous Galerkin time-domain method for HIRF assessment," *IEEE Trans. Electromagn. Compat.*, 2013, to be published. 2014
Q2 [7] G. G. Gutierrez, S. F. Romero, J. Alvarez, S. G. Garcia, and E. P. Gil, "On the use of FDTD for HIRF Validation and Certification," *PIERS Progr. Electromagn. Res. Lett.*, vol. 32, pp. 145–156, 2012.
[8] S. F. Romero, G. G. Gutierrez, A. L. Morales, and M. A. Cancela, "Validation procedure of low level coupling tests on real aircraft structure," in *Proc. Int. Symp. Electromagn. Compat. EMC Eur.*, 2012.
[9] I. Junqua, J.-P. Parmantier, and M. Ridel, "Modeling of high frequency coupling inside oversized structures by asymptotic and PWB methods," in *Proc. Int. Conf. Electromagn. Adv. Appl. ICEAA*, 2011.
[10] *"Guide to Certification of Aircraft in a High Intensity Radiated Field (HIRF) Environment,"* A ed., SAE ARP 5583, Jun. 2010.
[11] S. G. Garcia, J. Alvarez, L. D. Angulo, and M. R. Cabello. (2011) UGRFDTD EM solver. [Online]. Available: http://maxwell.ugr.es/ugrfdtd
[12] D. A. Hill, M. T. Ma, A. R. Ondrejka, B. Riddle, M. L. Crawford, and R. T. John, "Aperture excitation of electrically large, lossy cavities," *IEEE Trans. Electromagn. Compat.*, vol. 36, no. 3, pp. 169–178, Aug. 1994.
[13] D. Birreck, G. Guida, D. Marley, F. Marliani, S. Marra, and V. Martorelli, "Assessment of electromagnetic fields inside the communication module of a telecom satellite," presented at the ESA Workshop Aerospace EMC, Venice, Italy, 2012.
[14] *"Standard for Validation of Computational Electromagnetics Computer Modeling and Simulations,"* IEEE Standard 1597.1
[15] *"Metallic Materials and Elements for Aerospace Vehicle Structures,"* A ed., MIL-HDBK-5, Feb. 1966.
[16] E. P. Gil and G. G. Gutierrez, "Simplification and cleaning of complex CAD models for EMC simulations," presented at the Int. Symp. Electromagn. Compat. EMC Eur., York, U.K., 2011.
[17] K. S. Yee, "Numerical solution of initial boundary value problems involving Maxwell's equations in isotropic media," *IEEE Trans. Antenn. Propag.*, vol. AP-14, no. 3, pp. 302–307, May 1966.
[18] J. P. Bérenger, "A multiwire formalism for the FDTD method," *IEEE Trans. Electromagn. Compat.*, vol. 42, no. 3, pp. 257–264, Aug. 2000.
[19] GiD. (2010). "The personal pre and post processor." International Center for Numerical Methods in Engineering (CIMNE), Barcelona, Spain. [Online]. Available: http://www.gidhome.com
Q3 [20] NASH Mesher. Axessim. [Online]. Available: http://www.axessim.fr 2012
[21] A. Taflove, *Computational Electrodynamics: The Finite-Difference Time-*
Q4 *Domain Method*. Boston, MA: Artech, 1995.
[22] A. P. Duffy, A. J. M. Martin, A. Orlandi, G. Antonini, T. M. Benson, and M. S. Woolfson, "Feature selective validation (FSV) for validation of computational electromagnetics (CEM)—Part I: The FSV method," *IEEE Trans. Electromagn. Compat.*, vol. 48, no. 3, pp. 449–459, Aug. 2006.
[23] A. Orlandi, A. P. Duffy, B. Archambeault, G. Antonini, D. E. Coleby, and S. Connor, "Feature selective validation (FSV) for validation of computational electromagnetics (CEM)—Part II: Assessment of FSV performance," *IEEE Trans. Electromagn. Compat.*, vol. 48, no. 3, pp. 460–467, Aug. 2006.
[24] A. Orlandi, G. Antonini, C. Ritota, and A. Duffy, "Enhancing Feature Selective Validation (FSV) interpretation of EMC/SI results with Grade-Spread," in *Proc. IEEE Symp. Electromagn. Compat.*, Portland, OR, USA, 2006.
[25] R. Jauregui, F. Silva, A. Orlandi, H. Sasse, and A. Duffy, "Factors influencing the successful validation of transient phenomenon modelling," in *Proc. Asia-Pacif. Electromagn. Compat. Symp. Tech. Exhib.*, Beijing, China, 2010, pp. 2–5.
[26] FSV routine. [Online]. Available: http://ing.univaq.it/uaqemc/ 2010

Q5 **Guadalupe G. Gutierrez** was born in Leon, Spain, in 1979. She received the degree in physics in 2002 from the University of Salamanca, Salamanca, Spain. Since 2003, she has worked in different areas as EMC&MW Engineer at Airbus Military. Currently, her main activities concern electromagnetic simulations on aircrafts. M.Sc. degree

Jesus Alvarez (S'xx) was born in Leon, Spain. He received the B.Sc. degree in 2001 from the University of Cantabria, the M.Sc. degree from the University Carlos III of Madrid in 2008, and the Ph.D. degree from University of Granada in 2013, all in Spain. Q6

Since 2006, he has been with Cassidian, EADS-CASA, Spain, working as an Antenna and EMC Engineer. His current research interests include computational electrodynamics in time domain, method of moments and fast algorithms for integral equations in frequency domain and computational electromagnetic applied to electromagnetic compatibility, antenna, and RADAR cross-section problems. member of the IEEE since 2002

Enrique Pascual-Gil (M'xx) was born in Madrid, Spain, in 1964. He received the M.Sc. degree in aeronautic and computer sciences from Universidad Politécnica de Madrid (UPM), Madrid, Spain, in 1985 and 1997, respectively.

He has been working more than 25 years as EMC&MW Engineer in different areas. As the Head of Computational Electromagnetic at Airbus Military since 2008 being responsible of the electromagnetic simulation team dedicated to numerical modeling of all electromagnetic aspects of an aircraft, Airbus EMC Expert since 2011. He has participated as a Technical Manager in various national and international technology projects. His current interests include the application of numerical methods to solve more complex cases in order to achieve a complete virtual testing for aircraft certification.

Mauro Bandinelli was born in Italy in 1959. He received university degree (110/110 *cum laude*) in electronic engineering from the University of Florence, Florence, Italy, and the annual Italian Telecom Company award for his thesis work on "Numerical methods for antenna array design," in 1986. Q7 Q8

He is currently with the "Applied Electromagnetics Laboratory" and of the "Space Laboratory" at Ingegneria Dei Sistemi S.p.A, Pisa, Italy. His professional activity is focused on the development of numerical/asymptotic modelling methods and CAE tools for electromagnetic applications and on antenna design. He is the author and coauthor of about 70 original papers at international meetings and on technical journals.

Rodolfo Guidi was born in Italy in 1969. He received the Laurea degree in telecommunication engineering from the University of Pisa, Pisa, Italy, in 1995.

He has been with IDS Ingengeria dei Sistemi S.p.A, Pisa, since 1996 as an EMC Engineer in Electromagnetic Computational Laboratory. His research interests include the development of numerical codes to manage large and complex electromagnetics problem and the design of antennas for space applications.

Valerio Martorelli was born in Rome, Italy, in 1981. He received the Master's degrees in telecommunications engineering from the University of Roma Tor Vergata, Rome, in 2006.

Since 2008, he is a Systems Analyst in Ingegneria dei Sistemi S.p.A., Pisa, Italy, and works for the Computational EM Laboratory as Antenna Designer and Electromagnetic Analyst.

Mario Fernández Pantoja (SM'xx) received the B.S., M.S., and Ph.D. degree in 1996, and 2001, respectively, in electrical engineering from the University of Granada, Granada, Spain.

Between 1997 and 2001, he was an Assistant Professor at the University of Jaen, Jaen, Spain, and then he joined the University of Granada where, in 2004, he was appointed as an Associate Professor. He has been a Guest Researcher at Dipartimento Ingenieria dell'Informazione in the University of Pisa, Pisa, Italy, with the Antenna and Electromagnetics Group at Denmark Technical University, and with the CEARL at Pennsylvania State University, USA. His research interests include the areas of time-domain analysis of electromagnetic radiation and scattering problems, optimization methods applied to antenna design, Terahertz technology, and nanoelectromagnetics.

Miguel Ruiz Cabello was born in Granada, Spain. He received the B.Sc. and M.Sc. in physics in 2008 and 2010, respectively, from the University of Granada, where ~~Granadawhere~~ he is currently working toward the Ph.D. degree from the Department of Electromagnetism and Matter Physics. He is currently in his 2nd year Ph.D. working in HPC time domain solvers for electromagnetic analysis and design. He is participating in the 7PM EU project HIRF-SE as a developer of the UGRFDTD solver.

Salvador G. Garcia (M'xx) was born in 1966 in Baeza, Spain. He received the M.S. and Ph.D. degrees (with extraordinary award) in physics from the University of Granada, Granada, Spain, in 1989 and 1994, respectively.

In 1999, he joined the Department of Electromagnetism and Matter Physics, University of Granada as an Assistant Professor (qualified for Full Professor since 2012). He has published more than 50 refereed journal articles and book chapters, and more than 80 conference papers and technical reports, and participated in several national and international projects with public and private funding. He has received grants to stay as a Visiting Scholar at the University of Duisburg (1997), the Institute of Mobile and Satellite Communication Techniques (1998), the University of Wisconsin-Madison (2001), and the University of Kentucky (2005). His current research interests include computational electromagnetics, electromagnetic compatibility, terahertz technologies, microwave imaging and sensing (GPR), bioelectromagnetics, and antenna design.

QUERIES

Q1. Author: Please provide the citation of Fig. 2 in text. line 141

Q2. Author: Please update Ref. [6]. 2014

Q3. Author: Please check whether Ref. [19] is okay as set. It is OK.

Q4. Author: Please provide the year information in Refs. [20] and [26]. [20] 2012; [26] 2010

Q5. Author: Please specify the degree that author "Guadalupe G. Gutierrez" has received in the year 2002. M.Sc.

Q6. Author: Please provide the year in which the author "Jesus Alvarez" became a member of the IEEE. 2002

Q7. Author: Please provide the year in which the author "Mauro Bandinelli" and "Salvador G. Garcia" became a member of the IEEE. Mauro Bandinelli is not a member of the IEEE

Q8. Author: Please specify the degree and the year that author "Mauro Bandinelli" has received fom the university of Florence.

Master degree in 1986

Enrique Pascual-Gil is member of the IEEE since 2012.

Mario Fernández Pantoja is Senior Member of the IEEE since 2012 and Member since 1997.

Other corrections in:
- Fig. 1
- Miguel Ruiz Cabello's biography

HIRF Virtual Testing on the C-295 Aircraft: On the Application of a Pass/Fail Criterion and the FSV Method

Guadalupe G. Gutierrez, Jesus Alvarez, *Student Member, IEEE*, Enrique Pascual-Gil, *Member, IEEE*, Mauro Bandinelli, Rodolfo Guidi, Valerio Martorelli, Mario Fernandez Pantoja, *Senior Member, IEEE*, Miguel Ruiz Cabello, and Salvador G. Garcia, *Member, IEEE*

***Abstract*—In this paper, we show the application of numerical simulation for the virtual testing of a very complex system under high-intensity radiated fields (HIRF) conditions. Numerical results have been compared to measurements performed on a C-295 aircraft. The approach is based on the use of multiple tools for the preprocessing, computation, and postprocessing, all of them integrated under the same framework. This study is a part of the HIRF SE project, and the final step for the validation of the tools involved there, to introduce the use of simulation in the whole aircraft certification process in an HIRF environment. The main goal of the project is to provide the aeronautic industry with a numerical modeling computing framework, which could be used to predict the electromagnetic performance, and to carry out parametrical studies during the design phase, when changes are simpler and less costly. It could also lead in the future to a considerable reduction on the certification/qualification testing phase on air vehicles, to cross validate the results obtained from measurement and simulation providing best confidence in them, and to attain a more exhaustive analysis to achieve a higher level in the air vehicle safety.**

***Index Terms*—Electromagnetic (EM), electromagnetic compatibility (EMC), feature selective validation (FSV), finite difference time domain (FDTD), high-intensity radiated fields (HIRF), low-level swept fields (LLSF), oversized cavity theory (OCT), perfect electric conductor (PEC), radio frequency (RF), time domain analysis.**

I. Introduction

The increment in the use of electronics and complexity in modern aircrafts, and the expanded use of the spectrum worldwide, makes the topic of susceptibility under high-intensity radiated fields (HIRF) conditions a key issue for the certification of any air vehicle. The traditional approach to tackle this electromagnetic compatibility (EMC) problem is based mainly on testing. This approach presents some limitations due to the complexity of the systems, sizes, and strong requirements, defined in terms of frequency bands and electrical field levels [1]. The development of efficient algorithms and methods able to deal with electrically large structures, and the exponential growth of computational capabilities, make it possible to estimate transfer functions between incident electromagnetic (EM) fields and internal fields, or induced currents on bundles. This technology, not only can save a lot of time and cost in the certification process of an aircraft, but it can also be very useful during the whole life of a system; design, development, certification, upgrading or maintenance phases, increasing the safety of the current approach.

In this context, the European FP7 HIRF-SE project [2] is intended to provide the aeronautics industry with a synthetic environment integrated by a numerical simulation tool set (finite difference time domain (FDTD), method of moments (MoM), multitransmission line network (MTLN), material modeling tool (MMT), etc.), preprocessing tools, such as meshers, and postprocessing tools (FFT, filters, feature selective validation (FSV) tool, etc.). This project agglutinates 44 partners, including airframers, national certification agencies, test-houses, commercial and university software houses, etc. One output of the project is a group of tools that work inside the same framework providing two key capabilities. On one hand, the tools can exchange data to perform the different phases of a specific simulation. On the other hand, the results from each particular tool can be used as inputs for other solvers in order to perform a better suited simulation to take into account the complexity of a real scenario.

The frequency spectrum of HIRF threats ranges from 10 kHz–40 GHz. Below 400 MHz, the dominant effect comes from the excitation of airframe resonances, inducing currents on the cable bundles of the aircraft. The penetration of the electric field into the equipment bays via gaps, seams, RF transparent materials. and apertures in the airframe structure and equipment enclosures, begins to increase its influence above 100 MHz. This energy, coming from the bundles into the equipments in the first case, or EM fields at wavelengths comparable to the equipment sizes in the second one, interacts directly with the avionics, being a source of malfunctions.

Manuscript received July 25, 2013; revised September 30, 2013; accepted October 29, 2013. This work was supported by the funding from the European Community Seventh Framework Programme FP7/2007-2013, under Grant 205294 (HIRF SE project), from the Spanish National Projects TEC2010-20841-C04-04, CSD2008-00068, from the Junta de Andalucia Project P09-TIC-5327, and from the Granada Excellence Network of Innovation Laboratories (GENIL) project.

G. G. Gutiérrez and E. Pascual-Gil are with Airbus Military, EADS Construcciones Aeronáuticas S.A., 28906 Getafe, Spain (e-mail: Guadalupe.Gutierrez@military.airbus.com; Enrique.Pascual@military.airbus.com).

J. Alvarez is with the Cassidian, EADS Construcciones Aeronáuticas S.A., 28906 Madrid, Spain (e-mail: jesus@ieee.org).

M. Bandinelli, R. Guidi, and V. Martorelli are with the IDS, Ingegneria dei Sistemi, 56121 Pisa, Italy (e-mail: m.bandinelli@idscorporation.com; r.guidi@idscorporation.com; v.martorelli@idscorporation.com).

M. F. Pantoja, M. R. Cabello, and S. G. Garcia are with the Department of Electromagnetism, University of Granada, 18071 Granada, Spain (e-mail: mario@ugr.es; mcabello@ugr.es; salva@ugr.es).

Color versions of one or more of the figures in this paper are available online at http://ieeexplore.ieee.org.

Digital Object Identifier 10.1109/TEMC.2013.2291680

A validation road map has been defined inside the HIRF-SE project, to assess the capabilities of the different tools and methods, and to ensure their correct application. This road map is based on three levels. In the first level, numerical test cases have been defined and solved with different methods and tools, finding basically code-to-code cross comparison and validation [3]–[6]. The second step is based on checking the validity of the codes to simulate more complex test cases, some of them representing real configurations, such as aeronautic structures, materials and bundles, by comparing experimental data with numerical results [7]–[9]. And finally, the third level performs a final validation by comparisons of results on real air vehicle test cases, and also addresses the application of the HIRF-SE framework in a certification process.

In this study, we present the final step where some of the methods and tools, already validated at first and second levels under HIRF-SE, are applied on a real aircraft. For that purpose, we use the Airbus Military C-295, for which low-level swept fields (LLSF) measurements exist.[1] We compare with simulation results found with two numerical methods to address the full frequency band: the FDTD tool by the UGR (UGRFDTD) [11] for low and intermediate frequencies, and a power balance [12], [13] technique by IDS (IDSOCT) for high frequency. Results serve to validate the road map defined under the HIRF-SE project for HIRF assessment by numerical techniques. Whenever the simulation results are good or conservative, they could be used for reducing the amount of tests during a certification process.

The rest of the paper is organized as follows. First, a description of the C-295 aircraft and details about the starting point and available information is presented, regarding measurements and CAD information. Second, details about the EM numerical modeling of the problem are provided. Finally, we show a comparison of measurements and simulations, applying both HIRF-SE pass/fail criterion and the IEEE standard FSV method [14].

II. Description of the Problem

The C-295 aircraft is a medium-weight transport aircraft, certified FAR-25 by FAA, the DGAC and the INTA airworthiness authorities. The airframe structure is mainly metallic, providing the first layer of protection from external EM sources. Each individual conductive structure component is required to have a low-impedance electrical bond in order to maintain an electrically homogeneous structure. Leakage of EM fields and currents may still occur due to apertures around hatches, joints, hinges and use of nonconductive materials in components such as windows, radomes, and fairings.

[1] LLSF procedure is used to measure the transfer function relating external RF fields to the internal RF fields. The test is conducted for several aircraft orientations and field polarizations to produce the worst case of the transfer functions for the bay being illuminated. These transfer functions can then be scaled to predict the field environment when the aircraft is exposed to the appropriate external HIRF environment to assess whether the internal HIRF electric fields comply with the specifications for maximum levels of the integrated systems [1], [10].

Fig. 1. LLSF tests at airbus military open-area test-site facility.

Fig. 2. Electric field measurements during LLSF tests.

Q1

The materials in use in the C-295 aircraft are standard aeronautic materials. The main conductive materials used (compliant with [15]) are as follows:

1) aluminum alloys: 2024, 6061, 7075, 7050;
2) ferrous alloys: DAISI 4340, AISI 321, PH 13-8Mo;
3) titanium alloys: Ti6Al4V.

Additionally, composite materials are also used in the aircraft manufacturing such as carbon fiber and fiberglass (e.g., the radome is a *sandwich*-type structure with outer fiberglass laminates).

The LLSF test was performed in an open-area test-site (OATS) facility, by illuminating the aircraft with antennas for the frequency band between 100 MHz and 18 GHz. The aircraft is positioned in a location at least as far as 50 m from any source of electrical or electromechanical noise, and far away from any obstacle that can produce any undesired reflection (see Fig. 1).

A. Measurements

Measurements of LLSF according to EUROCAE ED-107 [1], [10] have been performed by Airbus Military personnel in their

OATS facility located in Getafe (Spain). It is a circular platform 90 m in diameter made of concrete with an embedded metallic ground plane.

Before the test, the electric field level has been measured at the observation points but without the aircraft, obtaining the calibration field level. Then, the aircraft has been placed at the OATS and the electric field level at six test points have been measured and normalized to the calibration field. Two test points are located in the cockpit, three in the cargo bay and one in the engine. Each zone has been illuminated from several angles and two polarizations so as to find the worst possible scenario, with regard to the energy coupling through apertures or slots. The worst case results from all illumination angles, both polarizations, and the points located at the same zone, have been calculated.[2] The attenuation transfer functions for each zone have been used to be compared with the simulation results.

B. CAD Data and Defeaturing

The model is obtained from the aircraft digital mock up. An image of the C-295 digital mock-up can be seen in Fig. 3(a). However, the complexity of the full CATIA (computer-aided three-dimensional interactive application, property of Dassault Systèmes) model is unaffordable and unnecessary for EM simulation purposes. Therefore, a simplification is needed to get a model simple enough to be meshed and computed, retaining all the internal/external details to be representative from the EM point of view. Taking that into account, the simplification is a crucial task consisting in the elimination of very small parts and details like holes, bolts, or nuts, or the redefinition of complex surfaces, for which the engineer experience plays a fundamental role [16]. Fig. 3(b) illustrates the result of the simplification process in the C-295 aircraft. Whereas the original model size is around 14 GB (unmanageable for an average PC), the simplified model is around 30 MB, small enough to be manipulated in a PC, and, at the same time, containing all the relevant details so as to be electromagnetically representative.

Since the C-295 aircraft is mainly made of metallic materials, it can be considered for EM simulations as perfect electric conductor (PEC) surfaces. Engine nacelles are made of a multilayered carbon fiber with aluminum foil which has been modeled as PEC with perfect continuity between panels, since it has a high shielding effectiveness, and the main entry points of these cavities are other than the connections between different pieces. The same approach has been considered for other parts made of carbon fiber or fiber glass with aluminum foil located in the center wing, the landing gear sponsons or small pieces in the stabilizers or wings. The total amount of composite materials composing the C-295 aircraft is no more than 20%. Dielectrics with no losses, such as fiberglass parts, have been eliminated from the EM model. For high-frequency simulations performed with OCT, some absorbing volumes have been introduced as a model for the seats in the cockpit, and for the nonmetallic pipes in the engine.

[2]This is the maximum value frequency-by-frequency of all the curves under consideration, resulting the envelope of all of them.

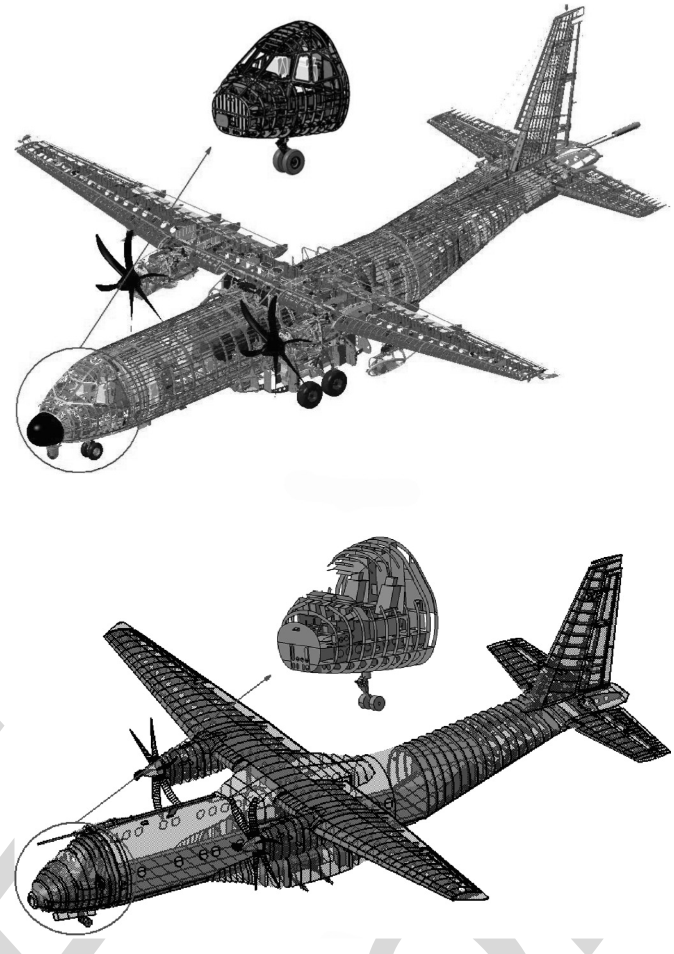

Fig. 3. (a) Isometric view of the C-295 digital mock-up with a detailed view of the cockpit. (b) C-295 simplified geometry with a detailed view of the cockpit (aerodynamic surfaces are depicted with a degree of transparency to allow the observation of the internal surfaces).

This simplified model made of metallic surfaces has been used for low-medium frequency simulations carried out with FDTD method between 100 MHz and 1 GHz. It has also been used in order to easily extract the volumes and surfaces required by power balance technique to perform high-frequency simulations between 1 and 18 GHz.

III. EM Modeling

Following the road-map defined inside the HIRF-SE project, numerical models of the C-295 aircraft have been prepared to work with the UGRFDTD code for low and medium frequencies and the IDSOCT code for high frequencies. A validation of the obtained results has been performed with respect to experimental data.

A. Low-Medium Frequency Model

The UGRFDTD [11] code has been used for simulating the frequency range between 100 MHz and 1 GHz. It is a time-domain 3-D full-wave method based in Yee classical FDTD method [17] with MTLN extensions for cable bundle treatment

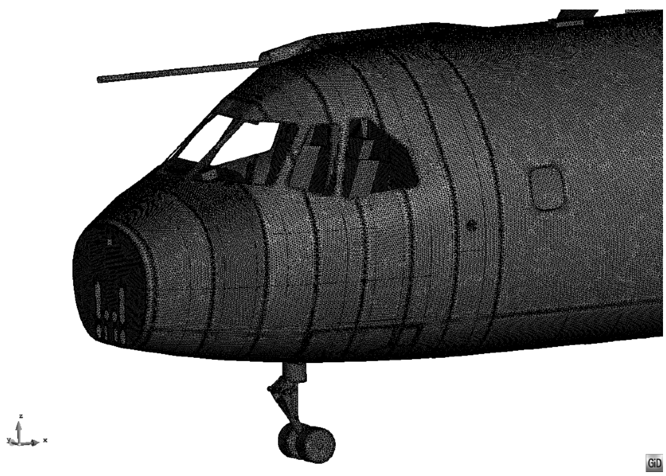

Fig. 4. C-295 cockpit unstructured mesh.

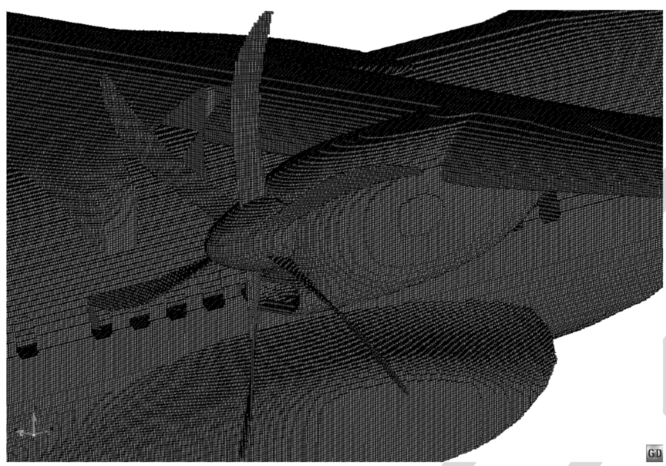

Fig. 5. Cartesian mesh of the engine and central fuselage external geometry.

[18]. The model has been built using GiD [19] and NASH [20] utilities. Further details of these (and other) tools used for the simulations are beyond the scope of this paper and provided in the references.

The first step consists on generating IGES files from the simplified CAD models, which are imported into GiD to obtain an unstructured mesh. In this case, a size of 20 mm has been used for the unstructured mesh.[3] A detailed view of the C-295 cockpit unstructured mesh appears in Fig. 4.

Second, from the unstructured mesh, a Cartesian mesh with uniform space steps in the three directions is created by using the NASH FDTD mesher. Reaching a compromise is necessary to select the cell size since it should be small enough to represent properly the relevant details of the structure and to solve the highest frequency of interest, and big enough to have a computationally affordable number of cells. In this case, a cell size of 20 mm has been selected, which has led to a total size of the grid of 734 Mcells (1228 $\times$ 1307 $\times$ 459). The quality of the Cartesian mesh can be seen in Fig. 5.

Finally, a simulation for each configuration is performed using the UGRFDTD code [11]. The time step has been selected at 80% of the Courant–Friedrichs–Lewy stability condition (30 ps) [21]. The space and time steps properly sample wavelengths and frequencies up to 1 GHz. The observables have been recorded for each time step. The boundary conditions have been set to perfect matching layer (PML) with eight cells, except for the lower Z-plane, where a PEC condition has been used to model the metallic ground plane of the OATS facility. The waveform of the plane wave illuminating the aircraft has been a modulated Gaussian pulse.

Taking into account the relationship between the distance from the illuminating antennas to the aircraft (10 m), and the size of the aircraft area being illuminated, the incident field can be considered to be in the far field for the measured frequency band (100 MHz to 18 GHz). Therefore a plane-wave illumination can be used instead of the actual test setup, with the subsequent computational resources savings (a deeper discussion on this is found in [7]).

B. *High-Frequency Model*

The IDSOCT code has been used for simulating the frequency range between 1 and 18 GHz. This method is based on oversized cavity theory (OCT) which belongs to the power balance approaches applicable to high-frequency modeling of quasi-cavity enclosures [12], [13].

Provided that some conditions about frequency, volumes, and Q factor of the enclosure are satisfied, it is demonstrated that the internal EM field distribution is statistically homogeneous, and follows some known statistical distributions (depending on the observable).

IDSOCT verifies the existence of such conditions in all different regions of the model, and calculates the parameters of the statistical distributions at them. From these, it is possible to extract the data of interest for the EMC problem. IDSOCT defines the characteristics of all the cavities in the aircraft including their volume, surface of the walls, surface of apertures, external sources, lossy objects, etc. In general, the cavities correspond to the different compartments of the aircraft. The panels represent the walls of those compartments. The apertures are the different holes, gaps, slots, etc., on the walls connecting a compartment to other ones, or to the exterior. And, the lossy objects replace the lossy materials existing within each compartment.

For the C-295 aircraft, all the geometrical parameters have been obtained from the simplified model using the measurement tools provided by CATIA V5. The resulting model comprises 17 cavities, 89 panels, 175 apertures, and 23 lossy objects. An external source corresponding to an impinging plane-wave of 1 V/m has been applied to each exterior aperture being illuminated from each illumination angle and field orientation, with respect to the apertures. The compartments where the field has been measured are the cockpit, the cargo bay, and the engine (the rest of the cavities have also been included, to take into account the connections between those ones, and/or to the exterior).

[3]Triangular elements are required (2087909 triangles in total) for PEC surfaces.

IV. Pass/Fail Criterion

A pass/fail criterion (PFC) has been defined within the project consortium, taking into account the expertise of certification authorities, airframers, test-houses, and simulation experts [1], [10], and [2]. The application of this criterion can be summarized as follows.

1) A set of seven observation points occupying the volume of the receiving antenna is used to probe the EM field through an average operation. This process obtains a better representation of the receiving antenna used during the tests.
2) A minimum of 100 frequencies per decade above 100 kHz equally spaced on a log scale is measured.
3) The raw data is filtered by using an averaging bandwidth of 5% of the frequency of interest.
4) The maximum value frequency-by-frequency considering all illumination angles and both polarizations, for each point, is calculated, and taken as the worst case (WC) results.
5) The maximum values of the WC, within a sliding frequency window of 10% of the central frequency, are used to find the data envelopes. This permits to account for any shift in resonances between the aircraft installation and the modeled test setup.
6) Finally, the value of the difference between simulation and measurement in dB is calculated.
7) The data are assumed to pass the criterion if this difference falls below 6 dB.

This PFC has been applied to the solvers developed under the HIRF-SE project in last validation phase, together with the FSV method (later presented), in order to perform cross comparisons and draw conclusions on their validity and range of application.

A. *PFC for Low-Medium Frequency*[4]

The numerical results for the E-fields at each test point have been normalized by the incident field of the plane-wave so as to obtain the attenuation transfer functions. Those results have been extrapolated to 1 V/m since the observables are the electric field normalized to an incident field of 1 V/m at each test point.

Figs. 6–8 show some comparisons between the WC results of the measured data and the ones of the numerical results using the UGRFDTD code, and also the comparison between the envelopes resulting from the application of the sliding frequency window. It can be seen that measurement and computation envelopes are less than 6 dB apart for most of the frequencies.

Table I summarizes the results for all the six points analyzed according to the PFC. The quality of the simulations can be considered good since the mean difference is close to 0 dB and the main deviations are located in narrow frequency bands [see Figs. 6 and 7(b)].

[4]For all the graphs shown in this section, the vertical scale has been removed due to nondisclosure and intellectual property rights (the missing *y*-axis are always linear with ticks spaced by 0.1 V/m).

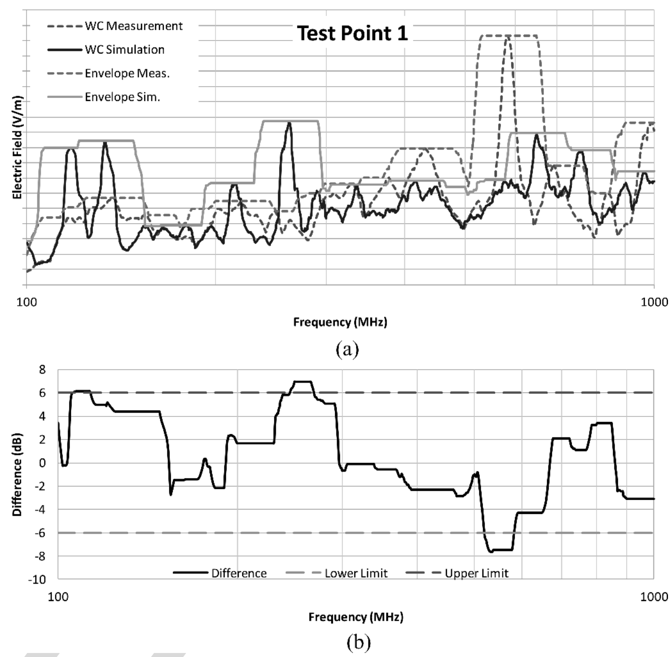

Fig. 6. (a) Comparison between measurements and simulations for the test point 1 located in the cockpit. (b) Difference between simulation and measurement and 6 dB limit.

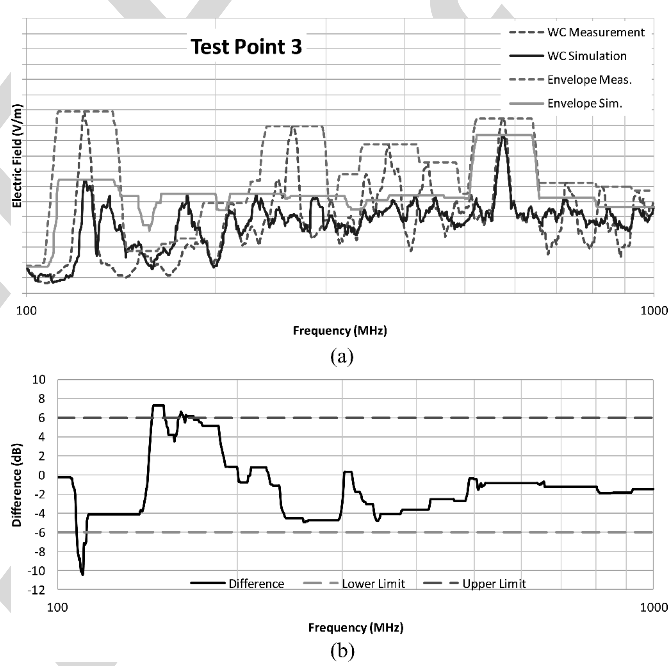

Fig. 7. (a) Comparison between measurements and simulations for the test point 3 located in the cargo bay. (b) Difference between simulation and measurement and 6 dB limit.

B. *PFC for High-Frequency Results*

For the high-frequency range, the shielding effectiveness at several points inside each cavity (for instance, the cockpit or the cargo bay) has been measured. Then, the mean values from all illumination angles, both polarizations and the points located at the same zone have been calculated and these transfer functions have been converted to E-field considering an illumination field

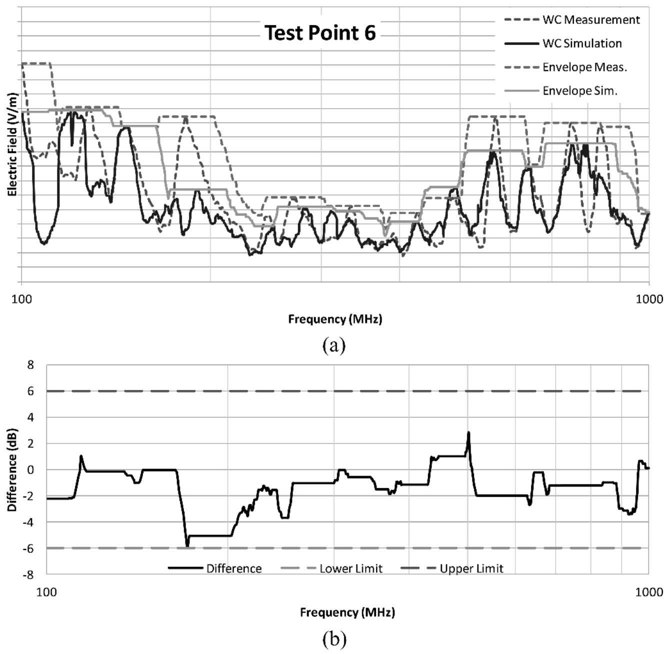

Fig. 8. (a) Comparison between measurements and simulations for the test point 6 located in the engine. (b) Difference between simulation and measurement and 6 dB limit.

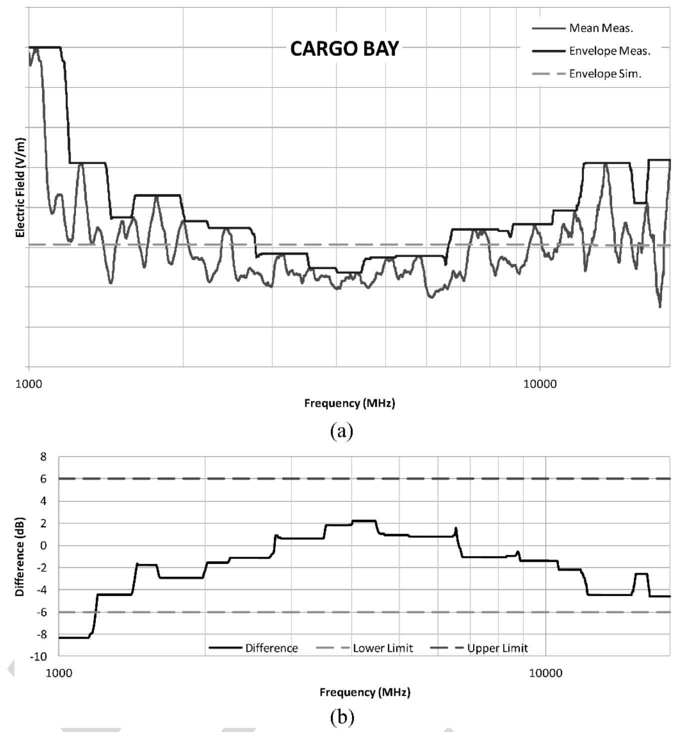

Fig. 9. (a) Comparison between measurements and simulations for the Cockpit. (b) Difference between simulation and measurement and 6 dB limit.

TABLE I
PFC Results for the UGRFDTD Code

Pass/Fail Criterion	*Points Inside Limit*	*Greatest Difference*	*Mean Difference*
Test Point 1	88 %	-7.65	0.51
Test Point 2	89 %	16.29	1.03
Test Point 3	94 %	-10.44	-1.34
Test Point 4	81 %	-14.41	-2.52
Test Point 5	76 %	-12.20	-1.55
Test Point 6	100 %	-5.95	-1.41

Percentage of points inside the limit, greatest difference between envelopes and mean difference between envelopes.

TABLE II
PFC Results for the IDSOCT Code

Pass/Fail Criterion	*Points Inside Limit*	*Greatest Difference*	*Mean Difference*
Cockpit	96 %	-6.98	-1.99
Cargo Bay	94 %	-8.33	-1.72
Engine	100 %	-5.48	-2.38

Percentage of points inside the limit, greatest difference between envelopes and mean difference between envelopes.

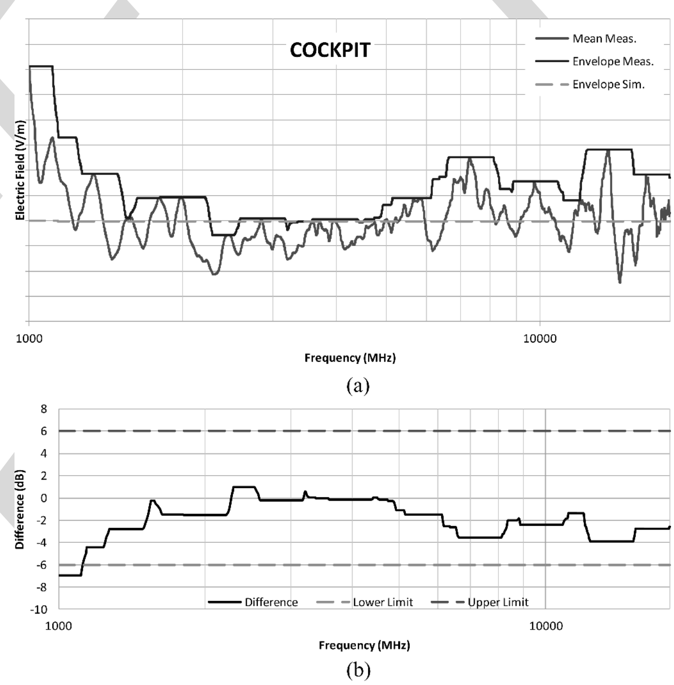

Fig. 10. (a) Comparison between measurements and simulations for the Cargo Bay. (b) Difference between simulation and measurement and 6 dB limit.

of 1 V/m. For the simulations, the mean E-fields at each cavity for an incident field of 1 V/m have been found using IDSOCT. The mean values from all illumination angles and polarizations have been computed.

Figs. 9–11 show the comparison between the mean and envelope measured values (with the procedure described for the PFC to find the envelopes) and the numerical results using the IDSOCT code.

Table II summarizes the results for the three zones under study. Similar conclusions that for the low-medium frequency case are found.

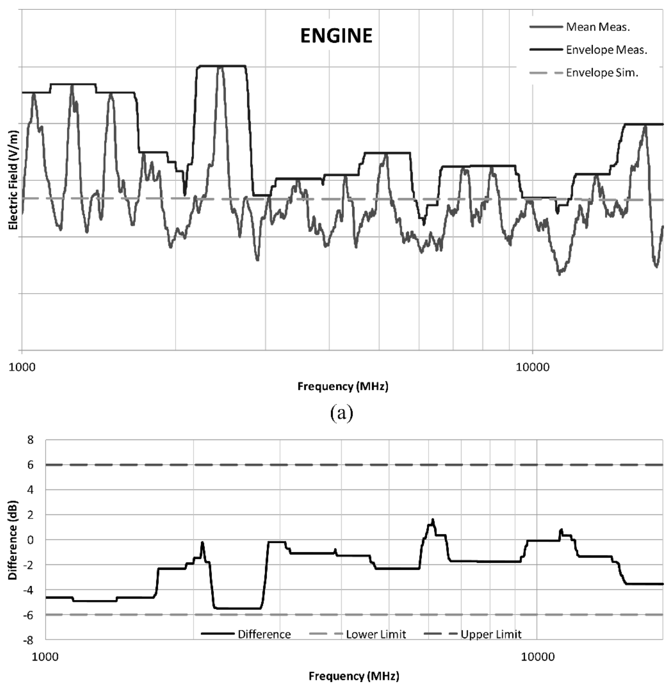

(a)

(b)

Fig. 11. (a) Comparison between measurements and simulations for the Engine. (b) Difference between simulation and measurement and 6 dB limit.

TABLE III
FSV Results for the UGRFDTD Code

FSV	GDM	ADM	FDM	Grade (G/A/F DM)	Spread (G/A/F DM)
Test Point 1	0.9936	0.6123	0.6880	5/5/5	3/4/5
Test Point 2	0.7764	0.4588	0.5796	5/4/5	4/4/5
Test Point 3	0.7689	0.4640	0.5572	5/5/5	4/4/5
Test Point 4	0.7943	0.5702	0.5042	5/5/5	3/4/5
Test Point 5	0.8357	0.4876	0.5682	5/5/5	4/5/5
Test Point 6	0.6295	0.3418	0.4934	5/4/5	4/4/5

V. Feature Selective Validation

One of the most widely used validation methods in EMC is the feature selective validation method (FSV) [22]–[25]. It was developed to take into account the expertise of engineers when assessing comparison of numerical/experimental data. It has been adopted by the IEEE standard 1597.1 [14]. In this paper, the FSV routine from the EMC Laboratory of the University of L'Aquila [26] has been used for this purpose.

The low-medium frequency simulation and measurement results have been analyzed with FSV. Fair agreements are obtained, in general, as seen in Table III. The actual WC curves have been employed now, instead of the envelopes used for the PFC, since they fit better to FSV methodology.

In order to provide a tentative correlation of the FSV and PFC ratings, let us use both methods to compare two sets of measurements, from two different test campaigns, performed with different C-295 aircrafts, and using different antennas and equipments. This comparison is helpful to find reference deviations in the comparison of two results. Fig. 12(a) depicts the result of the same data processing applied to two different attenuation measurements performed on a point in the cockpit.[5] Applying the PFC, the results shown in Fig. 12(b) and Table IV have been obtained, finding similar differences in both measurement/measurement and simulation/measurement comparisons in relation to the 6 dB limit.

The FSV rates for the measurement/measurement comparison are analyzed in Table V, revealing fair or even poor

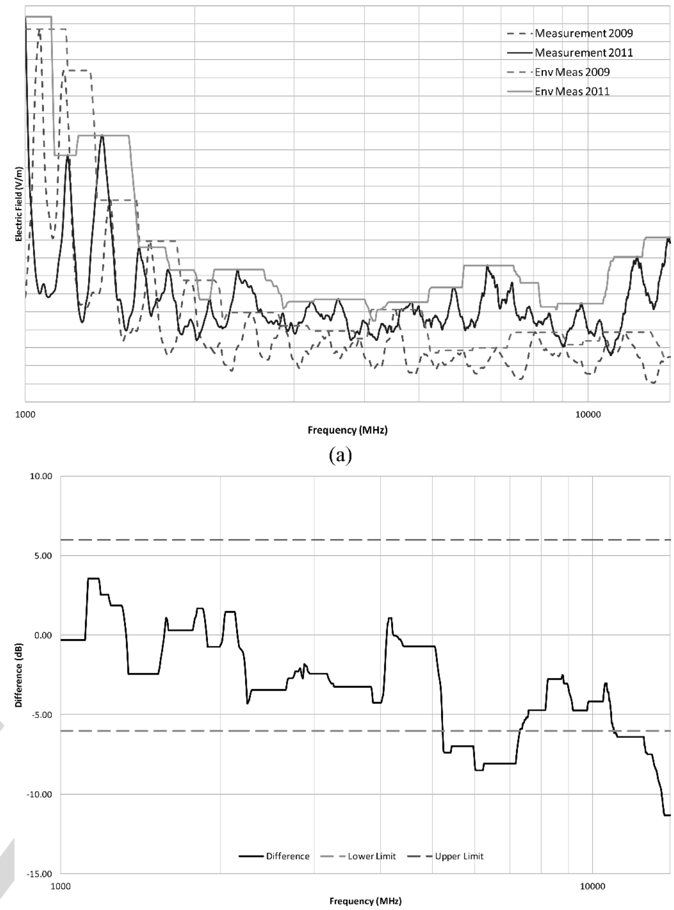

(a)

(b)

Fig. 12. (a) Comparison between two measurements on a point in the C-295 cockpit from different test campaigns. (b) Difference between the two measurements and 6 dB limit.

TABLE IV
PFC Results for Two Measurements From Different Test Campaigns

Pass/Fail Criterion	Points Inside Limit	Greatest Difference	Mean Difference
Point on cockpit	78 %	-11.33	-3.03

TABLE V
FSV Results for Two Measurements From Different Test Campaigns

FSV	GDM	ADM	FDM	Grade (G/A/F DM)	Spread (G/A/F DM)
Point on Cockpit	1.0232	0.8305	0.5663	5/5/5	3/3/5

[5]Only results for a single point in the cockpit were available to make this comparison (from 1000 to 14000 MHz).

agreement and high spread factors, as in the case of simulation/measurement comparison.

We can now extrapolate these PFC and FSV conclusions to the comparison of simulation with measurement data. For this case, like in the measurement/measurement one, fair or even poor agreement is found, while PFC finds matches within the 6 dB limit for most of the frequencies. It is inevitable to conclude that fair agreement for FSV could also be fully acceptable in both cases, since the uncertainty budget of simulations and measurements are in the same order of magnitude.

We must also note that the FSV results reveal a high spread factor for both comparisons. High values of spread factor are inherent in this kind of EMC comparisons for complex electrically large structures, with wide-frequency bands spanning over several decades. Wide typical deviations are due to the test procedure and the determination of the WC in shielding measurements. For this reason, we find points with excellent agreement, other ones with only good agreement and even points with poor agreement. A slight filtering is accepted by the standards, but the aim of the analysis is, generally, to capture the WC and not to average the results. Then, the comparisons must be made between curves with the aforementioned drawbacks.

VI. Conclusion

This paper shows a validation of a tool set that could help the aeronautical industry to predict the shielding effectiveness of aircrafts under HIRF conditions. Their application during the design, qualification, or certification phases, would lead to a significant reduction in both time and cost of the aircraft development, and to an improvement on the air vehicle safety.

Two numerical simulation tools (UGRFDTD and IDSOCT) have been validated using LLSF measurements for a complex aircraft (C-295). This test case is part of the final validation step of the HIRF-SE project, where most outstanding European airframers and EMC researchers participate. Both, the FSV method, and a novel PFC of ± 6 dB, for postprocessed raw data, to compare in terms of envelopes, have been employed and cross compared.

The hybrid approach presented in this paper, which is based on the combined use of an FDTD method for low-medium frequencies and a power balance technique for high frequencies, enables us to cover the whole frequency range required by HIRF certification authorities for LLSF test (from 100 MHz to 18 GHz). The use of the FDTD method can be extended up to higher frequencies depending on the available computational resources, hopefully up to frequencies for which the number of modes inside the geometry cavities is high enough to use the power balance technique with high accuracy. Then, the overlap of both methods permits us to predict the EM performance over the complete LLSF frequency band.

Simulation results show good agreement with measurements for those test points which are inside cavities with big apertures, where the main entry points are well defined, and the lossy objects are also well known. Differences found between 100 and 200 MHz are apparently due to the use of plane-wave illumination for this frequency range, where the far-field criterion is in its limit. In the high-frequency range, the deviations are located between 1 and 1.2 GHz because the number of modes inside the cavities at these frequencies is not high enough.

Regarding the PFC, we can state that, in general, the results differ less than 6 dB for most of the frequency range, as for the two measurements from different test campaigns. It means that 6 dB of difference is a tight requirement and the simulation results obtained in this study present good quality, and PFC is useful for validating the tools that have been used on a real and complex geometry.

As far as FSV method is concerned, both the quality and the reliability of the comparisons have been evaluated as low (since grade and spread factors are high) and the figures of merit show, in general, only fair agreement. Taking into account that it is also the case when comparing two measurements from different test campaigns, we can conclude that this kind of FSV results are inherent in that kind of EMC comparisons between wide frequency band signals, and therefore they can be very good results for that application.

The case analyzed in this paper has illustrated a correlation between the FSV method and the PFC, that may eventually help to revise the FSV standard, to provide rates closer to the experts evaluation for wide-frequency band EMC problems. Fair results with high spread factor have been proved to be acceptable in those applications. FSV would better mirror the PFC results by, for instance, giving less weight to the FDM value, even though ADM have high spread, and by giving more level of importance to the maximums when calculating the ADM.

The exercise shown in this paper is part of the demonstration of the utility and limits of numerical tools in HIRF assessment. It has provided a road map to create EM numerical models of test setups, suitable to replace some experimental testings by costless numerical simulations. The results of these validations are among to those currently being proposed to international aviation agencies to be accepted in certification air vehicles under HIRF conditions.

Acknowledgment

The authors would like to thank the whole HIRF-SE consortium, and especially those partners directly involved in the development of the PFC, used in this paper for the C-295 aircraft.

References

[1] *"Guide to Certification of Aircraft in a High Intensity Radiated Field (HIRF) Environment,"* EUROCAE ED-107, Mar. 2001.

[2] (2008). HIRF SE project. [Online]. Available: http://www.hirf-se.eu

[3] J. Alvarez, L. Angulo, M. Bandinelli, H. Bruns, M. Francavilla, S. Garcia, R. Guidi, G. Gutierrez, C. Jones, M. Kunze, J. Martinaud, I. Munteanu, M. Panitz, J. Parmantier, P. Pirinoli, Z. Reznicek, G. Salin, A. Schroder, P. Tobola, and F. Vipiana, "EV55: A numerical workbench to test TD/FD codes in HIRF EMC assessment," presented at the EUROEM Eur. Electromagn., Toulouse, France, 2012.

[4] J. Alvarez, L. Angulo, M. Bandinelli, H. Bruns, M. Francavilla, S. Garcia, R. Guidi, G. Gutierrez, C. Jones, M. Kunze, J. Martinaud, I. Munteanu, M. Panitz, J. Parmantier, P. Pirinoli, Z. Reznicek, G. Salin, A. Schroder, P. Tobola, and F Vipiana, "HIRF interaction with metallic aircrafts. A comparison between TD and FD methods," in *Proc. Int. Symp. Electromagn. Compat. EMC Eur.*, 2012.

[5] (2013). CEMEMC workshop. [Online]. Available: http://www.cememc.org

[6] J. Alvarez, L. D. Angulo, A. R. Bretones, and S. G. Garcia, "A leap-frog discontinuous Galerkin time-domain method for HIRF assessment," *IEEE Trans. Electromagn. Compat.*, 2013, to be published.

Q2 [7] G. G. Gutierrez, S. F. Romero, J. Alvarez, S. G. Garcia, and E. P. Gil, "On the use of FDTD for HIRF Validation and Certification," *PIERS Progr. Electromagn. Res. Lett.*, vol. 32, pp. 145–156, 2012.

[8] S. F. Romero, G. G. Gutierrez, A. L. Morales, and M. A. Cancela, "Validation procedure of low level coupling tests on real aircraft structure," in *Proc. Int. Symp. Electromagn. Compat. EMC Eur.*, 2012.

[9] I. Junqua, J.-P. Parmantier, and M. Ridel, "Modeling of high frequency coupling inside oversized structures by asymptotic and PWB methods," in *Proc. Int. Conf. Electromagn. Adv. Appl. ICEAA*, 2011.

[10] *"Guide to Certification of Aircraft in a High Intensity Radiated Field (HIRF) Environment,"* A ed., SAE ARP 5583, Jun. 2010.

[11] S. G. Garcia, J. Alvarez, L. D. Angulo, and M. R. Cabello. (2011) UGRFDTD EM solver. [Online]. Available: http://maxwell.ugr.es/ugrfdtd

[12] D. A. Hill, M. T. Ma, A. R. Ondrejka, B. Riddle, M. L. Crawford, and R. T. John, "Aperture excitation of electrically large, lossy cavities," *IEEE Trans. Electromagn. Compat.*, vol. 36, no. 3, pp. 169–178, Aug. 1994.

[13] D. Birreck, G. Guida, D. Marley, F. Marliani, S. Marra, and V. Martorelli, "Assessment of electromagnetic fields inside the communication module of a telecom satellite," presented at the ESA Workshop Aerospace EMC, Venice, Italy, 2012.

[14] *"Standard for Validation of Computational Electromagnetics Computer Modeling and Simulations,"* IEEE Standard 1597.1

[15] *"Metallic Materials and Elements for Aerospace Vehicle Structures,"* A ed., MIL-HDBK-5, Feb. 1966.

[16] E. P. Gil and G. G. Gutierrez, "Simplification and cleaning of complex CAD models for EMC simulations," presented at the Int. Symp. Electromagn. Compat. EMC Eur., York, U.K., 2011.

[17] K. S. Yee, "Numerical solution of initial boundary value problems involving Maxwell's equations in isotropic media," *IEEE Trans. Antenn. Propag.*, vol. AP-14, no. 3, pp. 302–307, May 1966.

[18] J. P. Bérenger, "A multiwire formalism for the FDTD method," *IEEE Trans. Electromagn. Compat.*, vol. 42, no. 3, pp. 257–264, Aug. 2000.

[19] GiD. (2010). "The personal pre and post processor." International Center for Numerical Methods in Engineering (CIMNE), Barcelona, Spain. [Online]. Available: http://www.gidhome.com

Q3 [20] NASH Mesher. Axessim. [Online]. Available: http://www.axessim.fr

[21] A. Taflove, *Computational Electrodynamics: The Finite-Difference Time-Domain Method*. Boston, MA: Artech, 1995.

Q4 [22] A. P. Duffy, A. J. M. Martin, A. Orlandi, G. Antonini, T. M. Benson, and M. S. Woolfson, "Feature selective validation (FSV) for validation of computational electromagnetics (CEM)—Part I: The FSV method," *IEEE Trans. Electromagn. Compat.*, vol. 48, no. 3, pp. 449–459, Aug. 2006.

[23] A. Orlandi, A. P. Duffy, B. Archambeault, G. Antonini, D. E. Coleby, and S. Connor, "Feature selective validation (FSV) for validation of computational electromagnetics (CEM)—Part II: Assessment of FSV performance," *IEEE Trans. Electromagn. Compat.*, vol. 48, no. 3, pp. 460–467, Aug. 2006.

[24] A. Orlandi, G. Antonini, C. Ritota, and A. Duffy, "Enhancing Feature Selective Validation (FSV) interpretation of EMC/SI results with Grade-Spread," in *Proc. IEEE Symp. Electromagn. Compat.*, Portland, OR, USA, 2006.

[25] R. Jauregui, F. Silva, A. Orlandi, H. Sasse, and A. Duffy, "Factors influencing the successful validation of transient phenomenon modelling," in *Proc. Asia-Pacif. Electromagn. Compat. Symp. Tech. Exhib.*, Beijing, China, 2010, pp. 2–5.

[26] FSV routine. [Online]. Available: http://ing.univaq.it/uaqemc/

Q5 **Guadalupe G. Gutierrez** was born in Leon, Spain, in 1979. She received the degree in physics in 2002 from the University of Salamanca, Salamanca, Spain. Since 2003, she has worked in different areas as EMC&MW Engineer at Airbus Military. Currently, her main activities concern electromagnetic simulations on aircrafts.

Jesus Alvarez (S'xx) was born in Leon, Spain. He received the B.Sc. degree in 2001 from the University of Cantabria, the M.Sc. degree from the University Carlos III of Madrid in 2008, and the Ph.D. degree from University of Granada in 2013, all in Spain. Q6

Since 2006, he has been with Cassidian, EADS-CASA, Spain, working as an Antenna and EMC Engineer. His current research interests include computational electrodynamics in time domain, method of moments and fast algorithms for integral equations in frequency domain and computational electromagnetic applied to electromagnetic compatibility, antenna, and RADAR cross-section problems.

Enrique Pascual-Gil (M'xx) was born in Madrid, Spain, in 1964. He received the M.Sc. degree in aeronautic and computer sciences from Universidad Politécnica de Madrid (UPM), Madrid, Spain, in 1985 and 1997, respectively.

He has been working more than 25 years as EMC&MW Engineer in different areas. As the Head of Computational Electromagnetic at Airbus Military since 2008 being responsible of the electromagnetic simulation team dedicated to numerical modeling of all electromagnetic aspects of an aircraft, Airbus EMC Expert since 2011. He has participated as a Technical Manager in various national and international technology projects. His current interests include the application of numerical methods to solve more complex cases in order to achieve a complete virtual testing for aircraft certification.

Mauro Bandinelli was born in Italy in 1959. He received university degree (110/110 *cum laude*) in electronic engineering from the University of Florence, Florence, Italy, and the annual Italian Telecom Company award for his thesis work on "Numerical methods for antenna array design," in 1986. Q7 Q8

He is currently with the "Applied Electromagnetics Laboratory" and of the "Space Laboratory" at Ingegneria Dei Sistemi S.p.A, Pisa, Italy. His professional activity is focused on the development of numerical/asymptotic modelling methods and CAE tools for electromagnetic applications and on antenna design. He is the author and coauthor of about 70 original papers at international meetings and on technical journals.

Rodolfo Guidi was born in Italy in 1969. He received the Laurea degree in telecommunication engineering from the University of Pisa, Pisa, Italy, in 1995.

He has been with IDS Ingengeria dei Sistemi S.p.A, Pisa, since 1996 as an EMC Engineer in Electromagnetic Computational Laboratory. His research interests include the development of numerical codes to manage large and complex electromagnetics problem and the design of antennas for space applications.

Valerio Martorelli was born in Rome, Italy, in 1981. He received the Master's degrees in telecommunications engineering from the University of Roma Tor Vergata, Rome, in 2006.

Since 2008, he is a Systems Analyst in Ingegneria dei Sistemi S.p.A., Pisa, Italy, and works for the Computational EM Laboratory as Antenna Designer and Electromagnetic Analyst.

Mario Fernández Pantoja (SM'xx) received the B.S., M.S., and Ph.D. degree in 1996, 1998, and 2001, respectively, in electrical engineering from the University of Granada, Granada, Spain.

Between 1997 and 2001, he was an Assistant Professor at the University of Jaen, Jaen, Spain, and then he joined the University of Granada where, in 2004, he was appointed as an Associate Professor. He has been a Guest Researcher at Dipartimento Ingenieria dell'Informazione in the University of Pisa, Pisa, Italy, with the Antenna and Electromagnetics Group at Denmark Technical University, and with the CEARL at Pennsylvania State University, USA. His research interests include the areas of time-domain analysis of electromagnetic radiation and scattering problems, optimization methods applied to antenna design, Terahertz technology, and nanoelectromagnetics.

Miguel Ruiz Cabello was born in Granada, Spain. He received the B.Sc. and M.Sc. in physics in 2008 and 2010, respectively, from the University of Granada, Granadawhere he is currently working toward the Ph.D. degree from the Department of Electromagnetism and Matter Physics. He is currently in his 2nd year Ph.D. working in HPC time domain solvers for electromagnetic analysis and design. He is participating in the 7PM EU project HIRF-SE as a developer of the UGRFDTD solver.

Salvador G. Garcia (M'xx) was born in 1966 in Baeza, Spain. He received the M.S. and Ph.D. degrees (with extraordinary award) in physics from the University of Granada, Granada, Spain, in 1989 and 1994, respectively.

In 1999, he joined the Department of Electromagnetism and Matter Physics, University of Granada as an Assistant Professor (qualified for Full Professor since 2012). He has published more than 50 refereed journal articles and book chapters, and more than 80 conference papers and technical reports, and participated in several national and international projects with public and private funding. He has received grants to stay as a Visiting Scholar at the University of Duisburg (1997), the Institute of Mobile and Satellite Communication Techniques (1998), the University of Wisconsin-Madison (2001), and the University of Kentucky (2005). His current research interests include computational electromagnetics, electromagnetic compatibility, terahertz technologies, microwave imaging and sensing (GPR), bioelectromagnetics, and antenna design.

QUERIES

Q1. Author: Please provide the citation of Fig. 2 in text.
Q2. Author: Please update Ref. [6].
Q3. Author: Please check whether Ref. [19] is okay as set.
Q4. Author: Please provide the year information in Refs. [20] and [26].
Q5. Author: Please specify the degree that author "Guadalupe G. Gutierrez" has received in the year 2002.
Q6. Author: Please provide the year in which the author "Jesus Alvarez" became a member of the IEEE.
Q7. Author: Please provide the year in which the author "Mauro Bandinelli" and "Salvador G. Garcia" became a member of the IEEE.
Q8. Author: Please specify the degree and the year that author "Mauro Bandinelli" has received fom the university of Florence.